General Disclaimer

One or more of the Following Statements may affect this Document

- This document has been reproduced from the best copy furnished by the organizational source. It is being released in the interest of making available as much information as possible.

- This document may contain data, which exceeds the sheet parameters. It was furnished in this condition by the organizational source and is the best copy available.

- This document may contain tone-on-tone or color graphs, charts and/or pictures, which have been reproduced in black and white.

- This document is paginated as submitted by the original source.

- Portions of this document are not fully legible due to the historical nature of some of the material. However, it is the best reproduction available from the original submission.

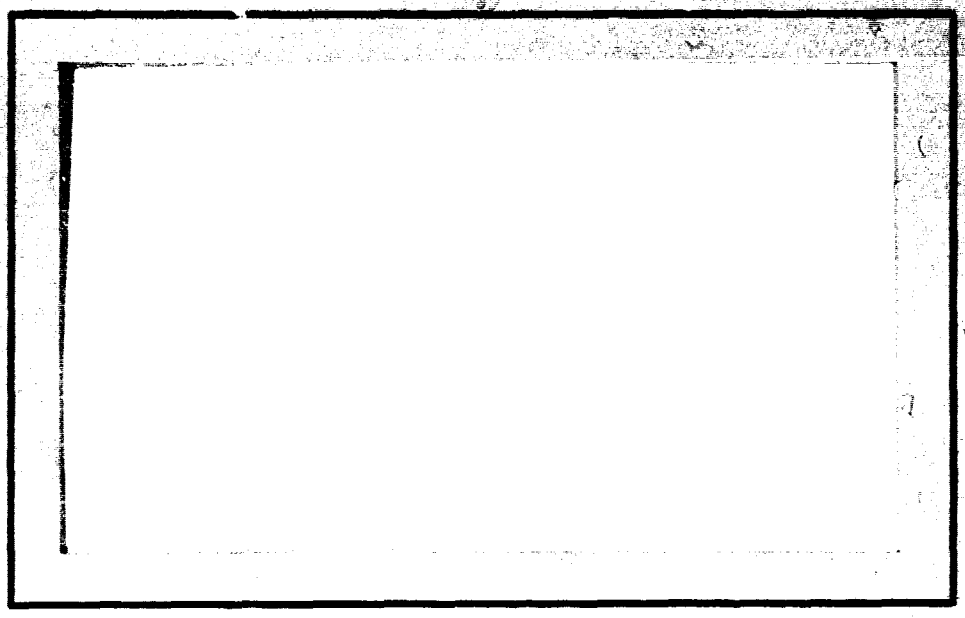

(NASA-CR-161526) SUPERCONDUCTING BEARINGS FOR APPLICATION IN CRYOGENIC EXPERIMENTS IN SPACE Final Report (Stanford Univ.) 65 p HC A04/MF A01 CSCL 13I

N80-28715

Unclas
G3/37 28266

High-Energy Physics Laboratory
W. W. Hansen Laboratories of Physics
STANFORD UNIVERSITY
STANFORD, CALIFORNIA

Final Report on Contract NAS8-32605 to Perform Laboratory Research On Superconducting Bearings for Application In Cryogenic Experiments in Space

Principal Investigator

C. W. F. Everitt

Associate Investigator

Paul W. Worden, Jr.

W. W. Hansen Laboratories of Physics

Stanford University

Stanford, California 94305

June 1980

I. INTRODUCTION

This research was conducted with the primary objective of developing and testing linear superconducting magnetic bearings suitable for use in a proposed orbital equivalence principle experiment and for general application in space. The particular bearings we have developed are cylindrical and designed for maximum stiffness radially and for minimum force and drag along the cylinder axis. The design is suitable for application to other geometries where maximum stiffness is desired. Under this contract we have perfected a working model scaled to operate in a 1-g environment, and have developed approximate solutions for the bearings which are easily applied to other situations.

The bearing we have developed is a critical component of a cryogenic equivalence principle experiment at Stanford.[1] In addition to the bearing research we have investigated some ancillary topics, in particular a superconducting transformer method of charging the magnets for the bearing, and a position detector based on a SQUID magnetometer and associated superconducting circuit. These devices are highly successful and, we believe, well understood.

II. DESCRIPTION OF APPARATUS

Figure 1 shows the concept of the bearing we have developed. Current flows in opposite directions in adjacent superconducting wires arranged parallel to the axis of a cylinder. This configuration provides maximum stiffness radially while allowing the test mass to move freely along the cylinder axis. In a space application the wires are extended to cover the entire perimeter of the cylinder: for the earth-based tests we have found it desirable to use only the bottom half. Control of the axial position of the test mass is by small control coils which may be positioned inside or outside the main bearing.

---

[1] P. W. Worden, Jr. 'Equivalence Principle Tests in Earth Orbit' Actra Astronautica, Vol. 5, pp. 27-42 (1978).

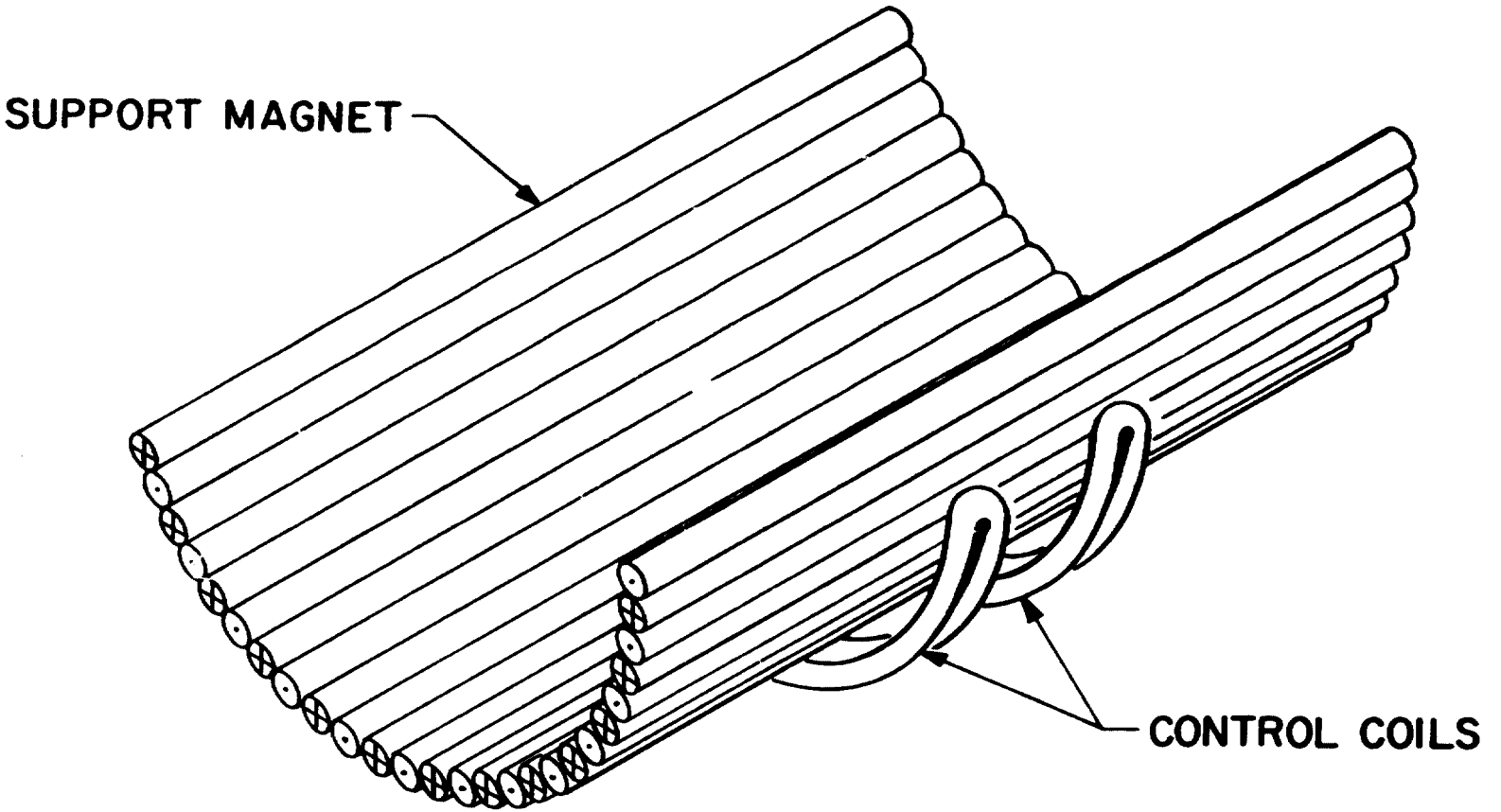

Figure 1

Concept of bifilar-wound bearing

The bearing is bonded to a rigid external support structure by a layer of expansion matched epoxy. The support structure for two concentric bearings is shown in Figure 2. This is the central apparatus for the earth-based equivalence principle experiment; it consists of a 1 cm. diameter and 5 cm. diameter bearing. This apparatus is presently made of copper. Not shown in figure 2 are the superconducting position detector coils near either end of each test mass, and the plates for the capacitance height detector above the outer test mass.

The main position detector circuit is shown in Figure 3. A SQUID magnetometer measures changes in a supercurrent caused by motions of a superconducting test mass. The circuit may be thought of as a DC inductance bridge in which two inductances are changed by the presence of the test mass. A magnetic field is trapped in a pair of superconducting coils; connected in parallel with them is a third coil coupled to the SQUID. Flux conservation in the superconducting circuit requires that a current flow in the third coil which is proportional to the displacement of the mass. We will discuss the sensitivity and limitations of this current below.

Vertical motions of the outer test mass can be measured with a pair of curved copper plates supported 0.3 mm. above the mass. The capacitance between these plates is changed by motion of the test mass; we were able to take position measurements up to 300 Hz by a fairly simple circuit that measures the RC time constant repetitively. The high frequency sensitivity is limited by vibrations in the relatively long, low capacitance leads used to connect to the capacitor plates. This device was also used as a horizontal position detector by offsetting the plates to one end of the test mass, with the advantage of being relatively linear and much less sensitive than the SQUID magnetometer.

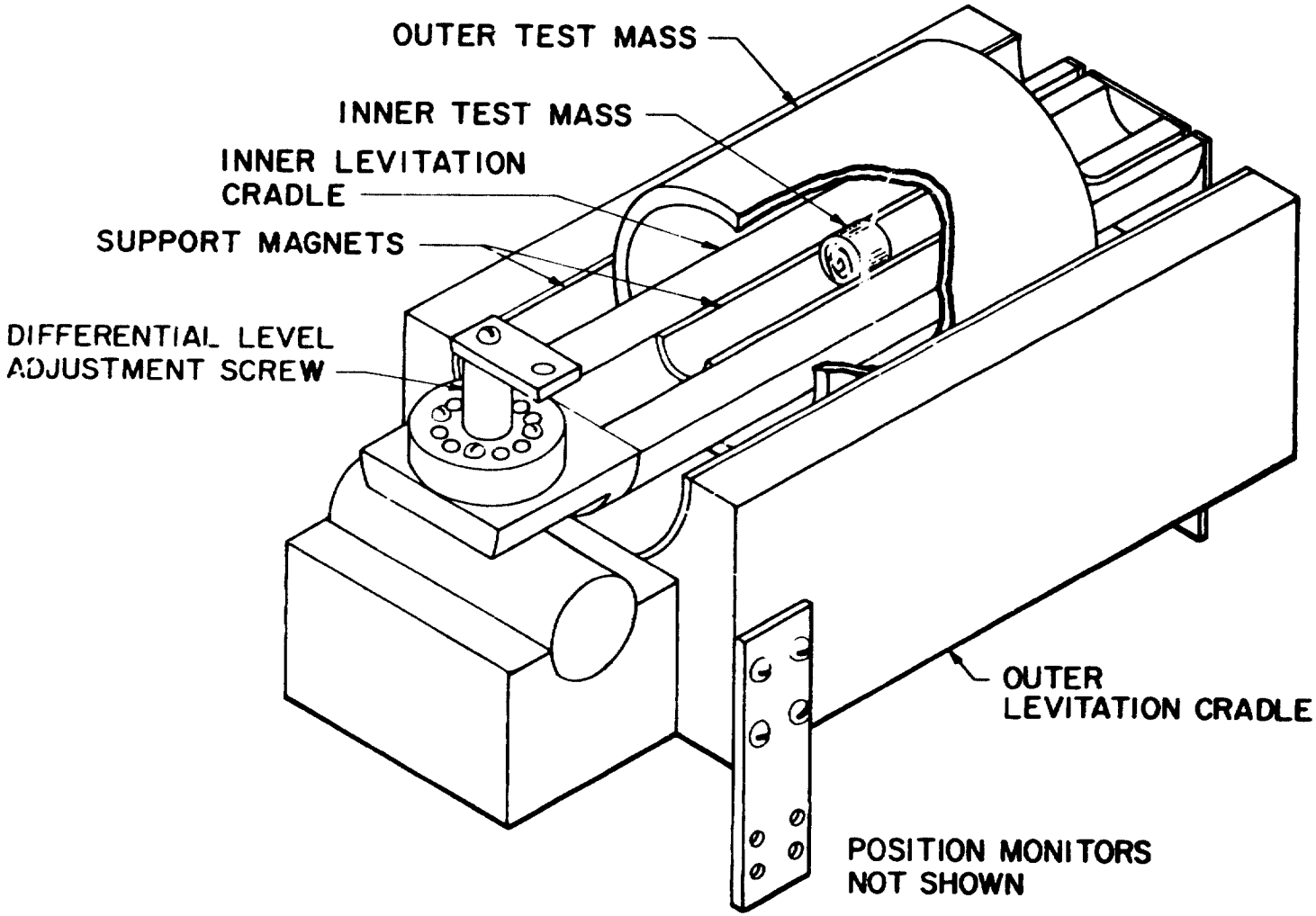

EQUIVALENCE PRINCIPLE ACCELEROMETER

Figure 2

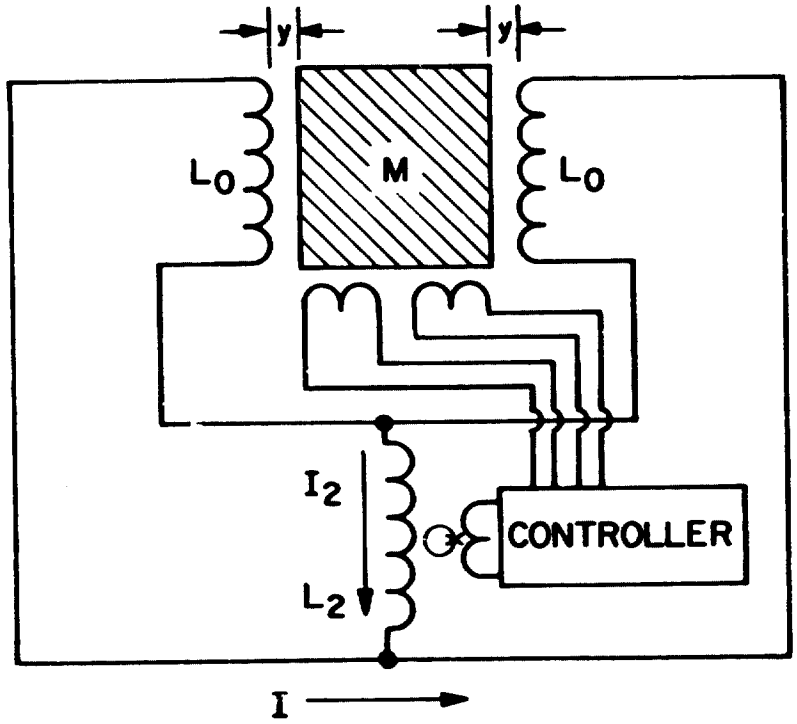

Figure 3

Superconducting Position Detector

The superconducting bearings are charged by superconducting flux transformers. This is necessary because the bearings require large currents to operate: a minimum of about 25 amperes. Busbars to carry this current would impose an unacceptable heat load on the helium bath, or would have to be detachable. With the flux transformers we are able to drive the bearings past their critical current ($\geq$ 60 amperes) with only 5 - 6 amps input in a single # 26 wire with the dewar probe providing the return path. An added benefit is that so little power is used that there is no risk of damaging the bearings or transformer if the critical current is exceeded.

The entire assembly is contained in a 12 inch diameter vacuum chamber on the end of a low temperature probe. In operation the probe is inserted into a helium dewar that is mounted so as to be tiltable over a range of about $\pm$ 1/4 degree. This allows levelling the apparatus to about 1 arc second, and since the mass controller circuits are not yet operational this has been the primary method of controlling the test mass position.

For the last six months we have been using a microcomputer system for data logging, with an enormous increase in quantity of data and quality of analysis over what we could do by hand. Initially we had only 8 bit A/D converters but in the last month we have increased the resolution to 16 bits. This puts the experimental sensitivity into an interesting range; we have the potential for much more improvement in sensitivity.

III . ANALYSIS OF BEARINGS

i. Requirements

A particular goal of this research has been the development of precision linear bearings for an equivalence principle experiment which is a working model of a proposed orbital experiment. The earth-based experiment is intended to develop the technology for the orbital version, and has as a design goal an acceleration sensitivity of 10^{-12} cm/sec^2, while the orbital experiment has a projected sensitivity of 10^{-14} cm/sec^2. The difference is due to the earth's large gravity field and seismic environment. Precise support and control of the test masses is necessary to make the experiment work.

There are four requirements on the suspension system for the test masses:[2]

1) It must be extremely stable. Changes in suspension characteristics may not be directly coupled into the measurement, but the differential measurement is extremely sensitive.

2) It must exert no strong forces in the sensitive direction. This would degrade the measurement by reducing the sensitivity to small forces.

3) It must have very low dissipation. Dissipation contributes directly to thermal noise, which is a limitation if the test masses are small.

4) It should have little intermode coupling. This is particularly important on earth, where nonlinear coupling may mix seismic noise into the longitudinal mode being used for the measurement.

The first and third requirements are automatically satisfied by a superconducting magnetic bearing. The stability of the superconducting magnet is probably limited mostly by its mechanical stability, which may be very high at low temperature.[3] For most practical purposes the dissipation is limited

---

[2] P. W. Worden, Jr., 'A Cryogenic Test of the Equivalence Principle', Stanford University Ph.D. Thesis (1976).

[3] Final Report on NASA Grant 05-02-019, "To Perform a Gyro Test of General Relativity in a Satellite and Develop Associated Technology", (C.W.F. Everitt Coordinator), W. W. Hansen Laboratories of Physics and Dept. of Aeronautics and Astronautics, Stanford University, Stanford, CA (July 1977) p. 210-223.

only by the gas in the system and the amount of normal metal present.

The second and fourth requirements may be satisfied by a good design. We decided on a cylindrical geometry for the apparatus. Each test mass is supported in a half-cylinder bearing or "levitation cradle" which ideally allows force-free motion along the cylinder axis and is very stiff radially - an upper half cylinder is redundant and counterproductive on earth. The difference in stiffness separates the normal mode frequencies and reduces coupling between them.

The design of the superconducting magnet which comprises the bearing was shown in figure 1; the considerations which led to it are given below. The "bifilar winding" of the magnet arranges that the current flows in opposite directions in adjacent wires, and provides the stiffest possible bearing. This is in contrast to the case where the currents all flow the same direction, which gives much less stiffness. The wires are parallel to the cylinder axis to reduce force variation along the axis. A pair of superconducting control coils allows small forces to be exerted on the test mass for centering and leveling. Many variations on the basic design are possible for different applications.

The bearings must exert axial forces small enough to allow measuring an acceleration of 10^{-12} cm/sec^2. The criterion is essentially that the variation of the bearing force be less than the desired sensitivity δa times the mass m of the test body; formally the sensitivity is

$$\delta a \geq \left(\frac{1}{\delta t^2} + \frac{1}{m} \frac{dF}{dx} \right) \delta x \qquad [1]$$

where δx is the least measurable displacement, δt is the time between measurements, and F is the extra force due to the bearing. In our case the mass is levitated in a gravitational field, and we can regard the extra force as due to the mass being raised or lowered by "bumps" in the imperfect bearing; other magnetic

forces, due for example to pinching of the sides of the bearing, will be the same order of magnitude. Therefore, $F = mg \frac{dh}{dx}$ where h is the height of levitation or variation from perfect straightness of the bearing. Since δt may be as long as we please, equation [1] reduces to a condition on the second derivative:

$$\frac{d^2h}{dx^2} < \frac{1}{g} \frac{\delta a}{\delta x} \qquad [2]$$

The quantities δa and δx are fixed by the experiment at 10^{-12} cm/sec^2 and 10^{-10} cm respectively; therefore, d^2h/dx^2 must be less than 10^{-5} cm^{-1}. This corresponds to about 0.05 cm of smooth variation per meter of length - a straightness equivalent to that of a good wooden ruler.

In space applications the requirement [2] can be significantly relaxed because g is very small. The bearing must be extended to a full cylinder to restrain the mass, and the appropriate parameter to use in place of g is the acceleration preload, that is, the acceleration g' that would be needed to hold the mass in place if half of the bearing were removed. For example, the orbital equivalence principle experiment might use a bearing with a preload of 10^{-2} cm/sec^2 with a position sensitivity of 10^{-10} cm. The derivative d^2h/dx^2 must be less than 10^{-2}.

The bearings for the earth bound experiment must have this straightness on a distance scale of the order of 1 mm and less. This rules out all bearings except those with wires parallel to the cylinder axis: a solenoidal winding, for example, has bumps in the magnetic field associated with individual wires. Even with wires parallel to the axis, care must be taken to use magnetically homogenous materials to support them. As we discovered for the inner levitation cradle, small particles of iron can produce bumps in the bearing which are much worse than the condition $d^2h/dx^2 < 10^{-5}$ cm^{-1}. Surface effects will also influence the bearing.

ii. Theoretical Treatment

The general concept of the magnetic bearings we have developed was shown in Figure 1. The particular configuration is optimized for use in earth's 1-g experiment; a general analysis for scaling them to other configurations and environments is given below, followed by some particular cases. As previously mentioned, the bifilar design we prefer maximizes radial restoring forces while minimizing axial forces. We include some analysis of other designs.

a) Nearly Exact Solution

In this treatment end effects due to the finite length of the wires are neglected; if the bearing is somewhat longer than the test mass and the bifilar winding scheme (Section IV below) is used, the end effects may be very small. We start by presenting the magnetic field B on a thin wire carrying a current I_j near a superconducting cylinder of radius a (fig. 4). The polar coordinates of this wire are (r_j, θ_j). Each wire I_i has two images in the cylinder: one of magnitude $-I_i$ at $(a^2/r_i, \theta_i)$ and one of magnitude $+I_i$ at the origin. We can ignore the force on the wire due to other wires in the bearing (since it is a rigid structure) and so we need to consider only the magnetic fields from the images of the array of wires. The field at wire j due to a single pair of images (of the ith wire) is most usefully expressed in cartesian components

$$B_x^{ji} = \frac{2I_i}{C}\left(-\frac{r_j\cos\theta_j - (a^2/r_i)\cos\theta_i}{r_j^2 + (a^2/r_i)^2 - \frac{2a^2 r_j}{r_i}\cos(\theta_j-\theta_i)} + \frac{\cos\theta_j}{r_j}\right) = \quad [3]$$

$$B_y^{ji} = \frac{2I_i}{C}\left(-\frac{r_j\sin\theta_j - (a^2/r_i)\sin\theta_i}{r_j^2 + (a^2/r_i)^2 - \frac{2a^2 r_j}{r_i}\cos(\theta_j-\theta_i)} + \frac{\sin\theta_j}{r_j}\right)$$

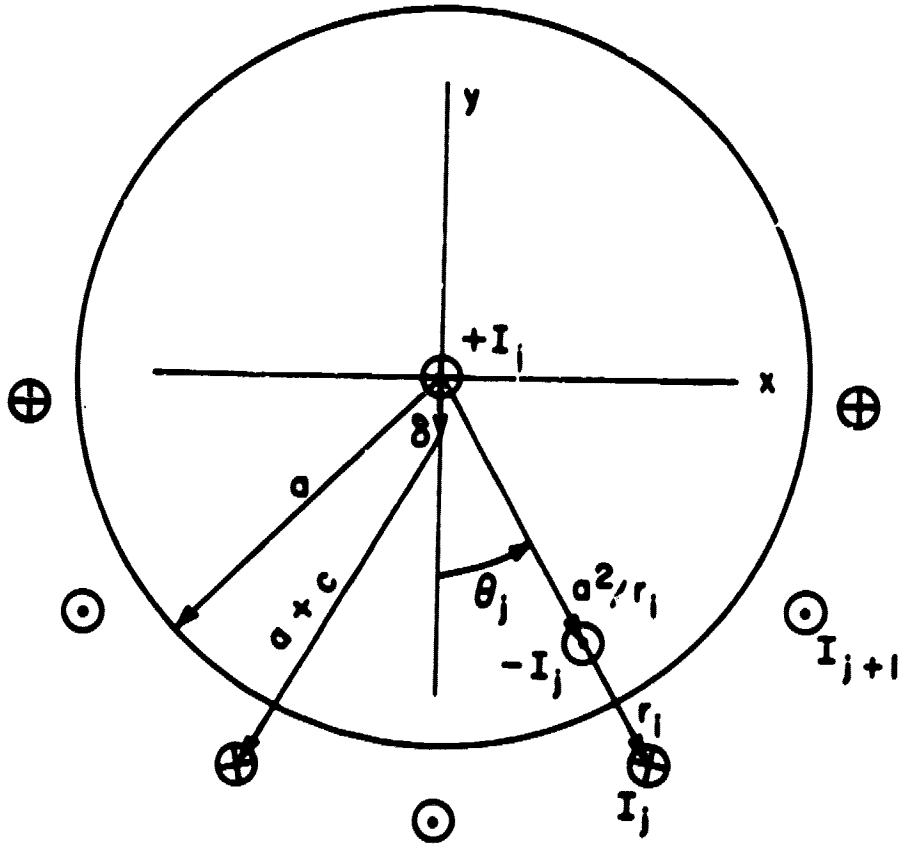

Figure 4

Geometry for force calculation

The total field at the jth wire due to the images of all wires is just the sum of the fields. If the number of wires is even, the total contribution from the central images is zero (since current flows opposite directions in adjacent wires, $I_i = (-1)^i I$).

$$B_x^j = \sum_i B_x^{ii} = -\frac{2I}{C} \sum_i (-1)^i \frac{(r_j \cos\theta_j - p_i \cos\theta_i)}{r_j^2 + p_i^2 - 2 r_j p_i \cos(\theta_j - \theta_i)} \qquad [4]$$

$$B_y^j = \sum_i B_y^{ji} = -\frac{2I}{C} \sum_i \frac{(-1)^i (r_j \sin\theta_j - p_i \cos\theta_i)}{r_j^2 + p_i^2 - 2 r_i p_i \cos(\theta_j - \theta_i)}$$

where $p_i = a^2/r_i$.

We are interested principally in the vertical component of force on the test mass. This is equal and opposite to the sum of the forces on the wires, or

$$F_y = -\sum_j \frac{I_Z}{C} \times B_x^j = \frac{2I^2}{c^2} \sum_j \sum_i (-1)^j (-1)^i \frac{(r_j \cos\theta_j - p_i \cos\theta_i)}{r_j^2 + p_i^2 - 2 r_j p_i \cos(\theta_j - \theta_i)} \qquad [5]$$

In this form the force may be accurately determined by numerical calculation but algebraic manipulation becomes unproductive.

Figures 5A, B and C show the results of numerical calculations for a 5 cm diameter bearing of 180 wires - approximately the same dimensions as the present outer bearing. The vertical axis should be multiplied by $2I^2/c^2$ to get the force per unit length in dynes; the horizontal axis is displacement as a fraction of the difference between the radius of the test mass and the radius of centers of the wires comprising the bearing.

Figure 5A

Vertical Force/ Unit Length of Half-Cylinder Bearing
as a function of normalized vertical displacement

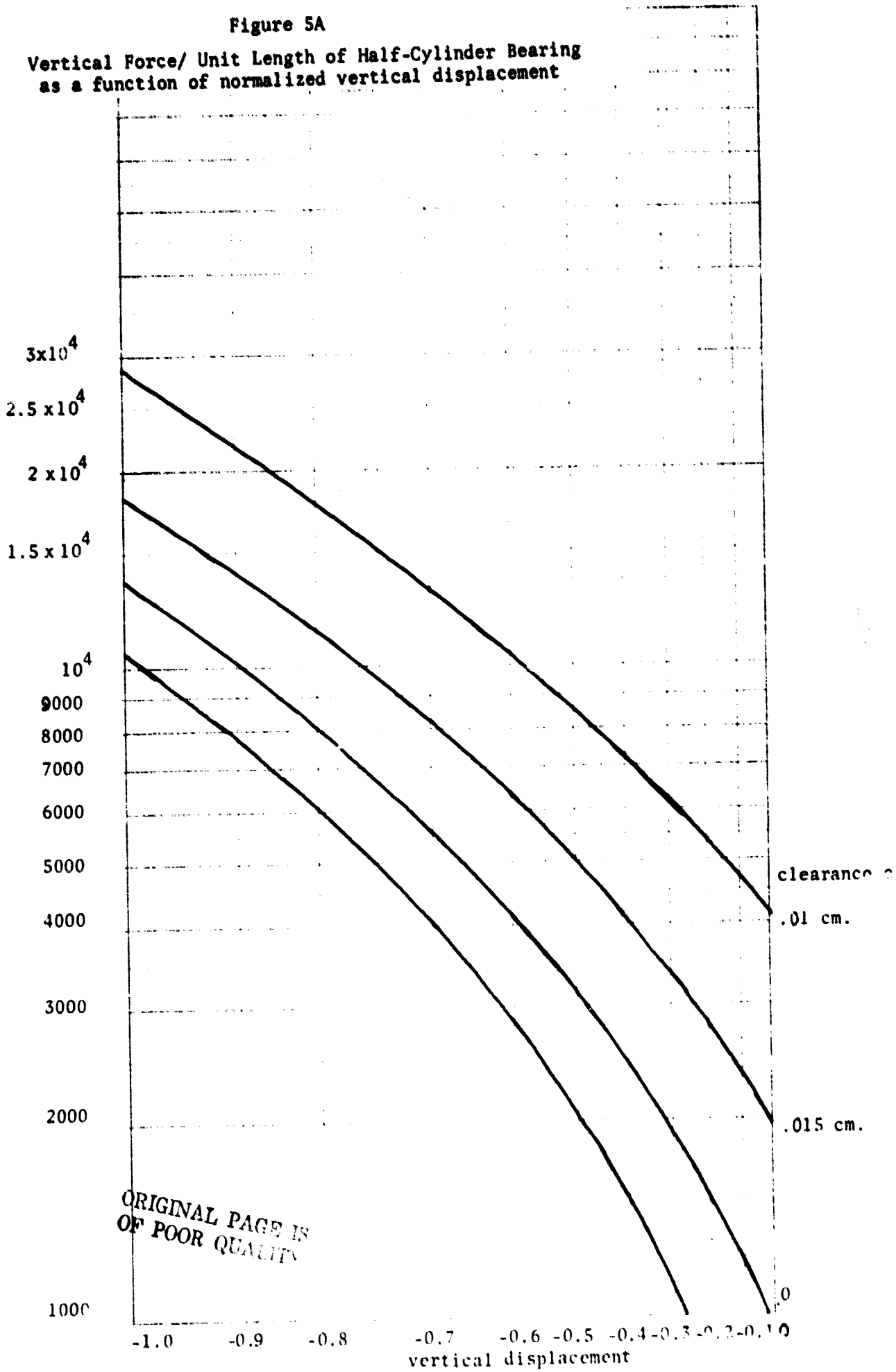

Figure 5B

Horizontal Restoring Force/Unit Length of Half-cylinder Bearing
as a function of normalized horizontal displacement

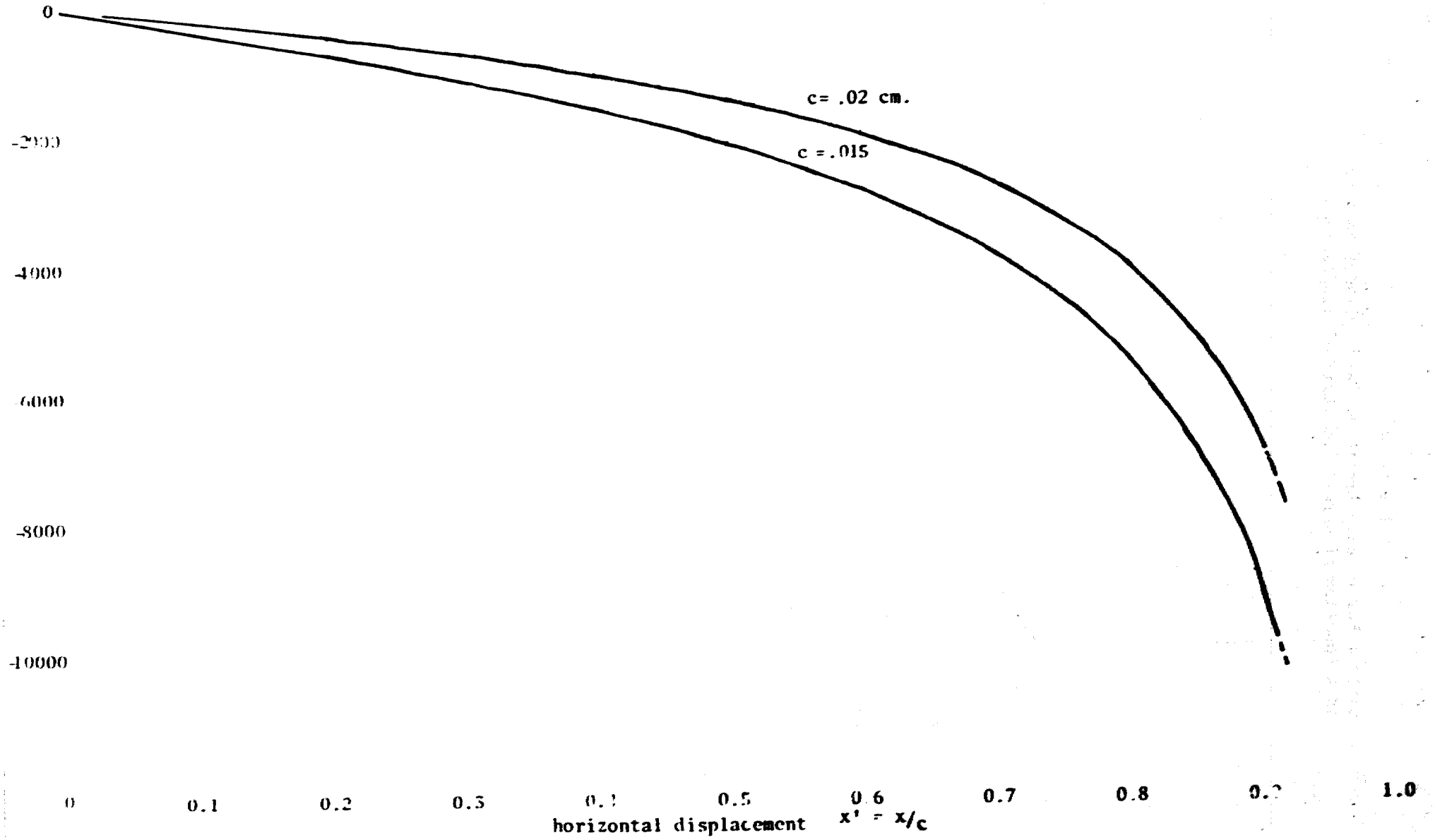

Figure 5C

Variation in Vertical Force/Unit Length
as a function of horizontal displacement

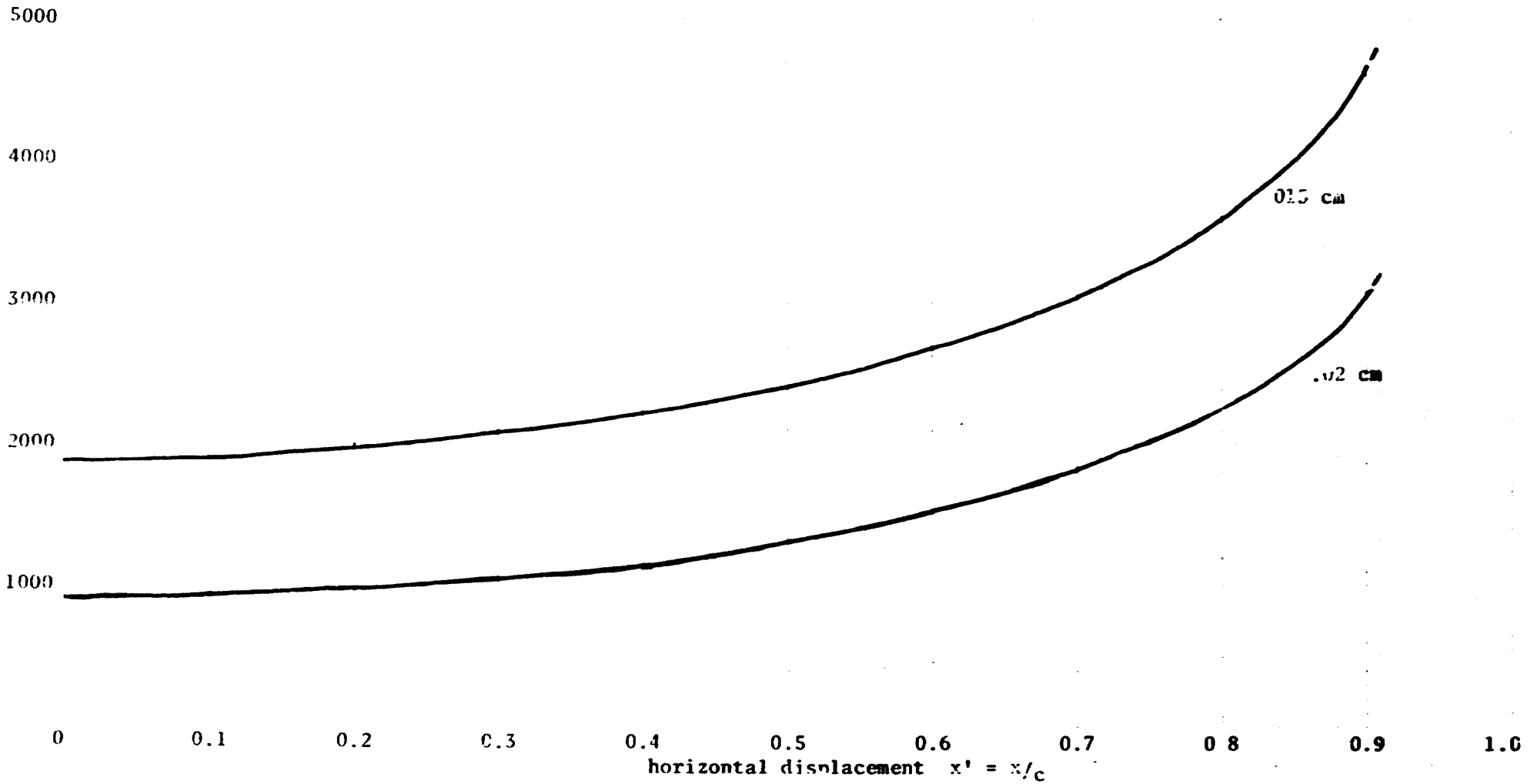

b) Locally flat Approximation

A second method of approximating the force is to assume that the wires are spaced closely enough that any global curvature is negligible. The bearing then looks like a plane array of wires parallel to the Z-axis and with spacing $2s > r$ along the x-axis (Fig. 6). The mass is at height $h > r$ above the centers of the wires. The force on the ith wire due to images of all wires is given by

$$F_i = \frac{2I_i}{c^2}\,\frac{h}{2s^2}\sum_i \frac{I_j}{(n/s)^2+j^2} \qquad [6]$$

If $I_j = (-1)^j I$ the force for an infinite array is

$$F_i = \frac{I^2}{c^2}\left[\frac{2h}{s^2}\sum_{j=1}^{\infty}\frac{(-1)^j}{(h/s)^2+j^2} + \left(\frac{s}{h}\right)^2\frac{h}{s^2}\right]$$

$$= \frac{I^2}{c^2}\,\frac{\pi}{s}\,\frac{1}{\sinh(\pi h/s)} \qquad [7]$$

If there are $N = \frac{1}{2s}$ wires per unit distance the force per unit area is

$$F = NF_i = \frac{\pi I^2}{2c^2}\,\frac{1}{s^2}\,\frac{1}{\sinh(\frac{\pi h}{s})} \qquad [8]$$

Another interesting case is that where the currents are parallel, i.e., $I_i = I$ for all I: the case in a long solenoid for example. The force on the ith wire becomes

$$F_i = \frac{I^2}{c^2}\,\frac{1}{s}\,2\,\frac{h}{s}\sum_{j=1}^{\infty}\frac{1}{\left(\frac{h}{s}\right)^2+j^2} + \frac{s}{h} \qquad [9]$$

$$= \frac{I^2}{c^2}\cdot\frac{\pi}{s}\coth(\pi h/s).$$

There is an important contrast between equations [7] and [9] in the limit as the height becomes much more than the spacing between the wires. For h/s

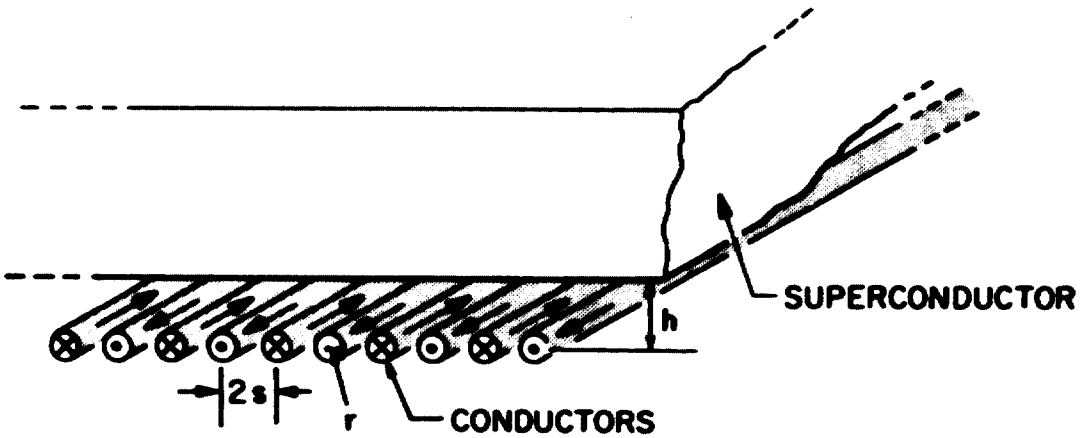

Figure 6
Locally flat geometry

large equation [7] tends to 0 as $e^{-\pi h/s}$; equation [9] tends to a constant force. Equally important is the behavior of the force gradient, which determines the resonant frequency. The gradient of [7] for large h/s is proportional to $e^{-\pi h/s}$, while that of [9] is proportional to $e^{-\frac{2\pi h}{s}}$. The significance of this is that in this approximation parallel currents give the larger force, but antiparallel currents will always give a larger force gradient and hence a higher resonant frequency. It is important in the equivalence principle experiment to ensure separation of normal mode frequencies to prevent problems with nonlinear coupling, and we therefore chose antiparallel currents, and accepted the smaller lift force and close tolerances necessary.

For a given height h there is an optimum spacing which gives a maximum force per unit area. Differentiation of [7] with respect to s gives the condition $\frac{\pi h}{2s} \cosh\left(\frac{\pi h}{s}\right) = \sinh\left(\frac{\pi h}{s}\right)$ which has the solution $(h/s)_{opt.} = 0.609566$. Thus the spacing of wires which are optimally spaced at liftoff ($h = d/2$) is $2s = 1.6405\ d$. There is an optimum diameter of the wire for a given spacing which is less useful. Generally the critical current of a superconducting wire in a small magnetic field is proportional to its cross-section, i.e., $I_c = \lambda d^2$, so that $F_{max} = \frac{\pi \lambda^2 d^4}{c^2 s^2} \frac{1}{\sinh(\pi d/2s)}$. Here the maximum force is at the position $h = d/2$, where the mass is just touching the supporting wires. The optimum comes at $s \approx 0.393\ d$, requiring the wires have a larger diameter than their spacing allows. If critical current is a limiting factor the wires should have as large a diameter as possible.

With the approximation (7) we can calculate the total lift force by integrating over the area. The total vertical force per unit length is

$$F_1 = \int_{-\pi/2}^{\pi/2} F\cos\theta r d\theta = \int_{-\pi/2}^{\pi/2} \frac{\pi I^2}{2c^2 s^2} \frac{r}{\sinh(\frac{\pi h}{s})} \cos\theta \, d\theta$$

$$= \frac{\pi I^2 r}{c^2 s^2} \int_0^{\pi/2} \frac{\cos\theta \quad d\theta}{\sinh(\frac{\pi c}{s} - \frac{\pi\delta\cos\theta}{s})} \qquad [10]$$

where now $h = c - \delta\cos\theta$, and r is the radius of the bearing.

With the approximation $\sinh(\pi\frac{h}{s}) \approx e^{\lambda h/s}$ this expression can be integrated in terms of modified Struve functions and Bessel functions. It is more useful to do a numerical integration. The result is in Figures 7A and 7B. These are normalized so that the maximum support force ($\delta = c$) is unity, and the height $\delta' = \delta/s$ and clearance $x_o = c/s$ are normalized by the wire spacing. Over most of the range of interest ($\delta' < 1$) the force decreases approximately exponentially. The resonant frequencies of several idealized situations are easy to calculate. For large x, $\sinh(x) \cong \frac{1}{2}e^x$; therefore for a mass m of area A levitated near an infinite plane array of wires, the total force is approximately $F = \frac{A\pi I^2}{2c^2 s^2} e^{-\pi h/s} - mg$. The spring constant at the equilibrium height h_o is $k = -\frac{df}{dx} = \frac{\pi}{s} \cdot \frac{A\pi I^2}{2c^2 s^2} e^{-\pi h_o}$. But the equilibrium height h_o is defined by $\frac{A\pi I^2}{2c^2 s^2} e^{-\pi h_o/s} = mg$, and since $\omega_o^2 = k/m$, the resonant frequency is given by

$$f = \frac{1}{2\pi} \left(\frac{\pi g}{s}\right)^{\frac{1}{2}} . \qquad [11]$$

This depends only on the wire spacing and external gravitational field: the mass settles to an equilibrium position where the force gradient is proportional to the weight of the mass, because of the exponential form of the force. It is true of many of the levitation schemes with antiparallel currents that the vertical period in a gravitational field does not depend strongly on the height of the levitation, for the same reason. The variation of frequency

Figure 7A

Fraction of total support force as a function of normalized height δ' and clearance x_o

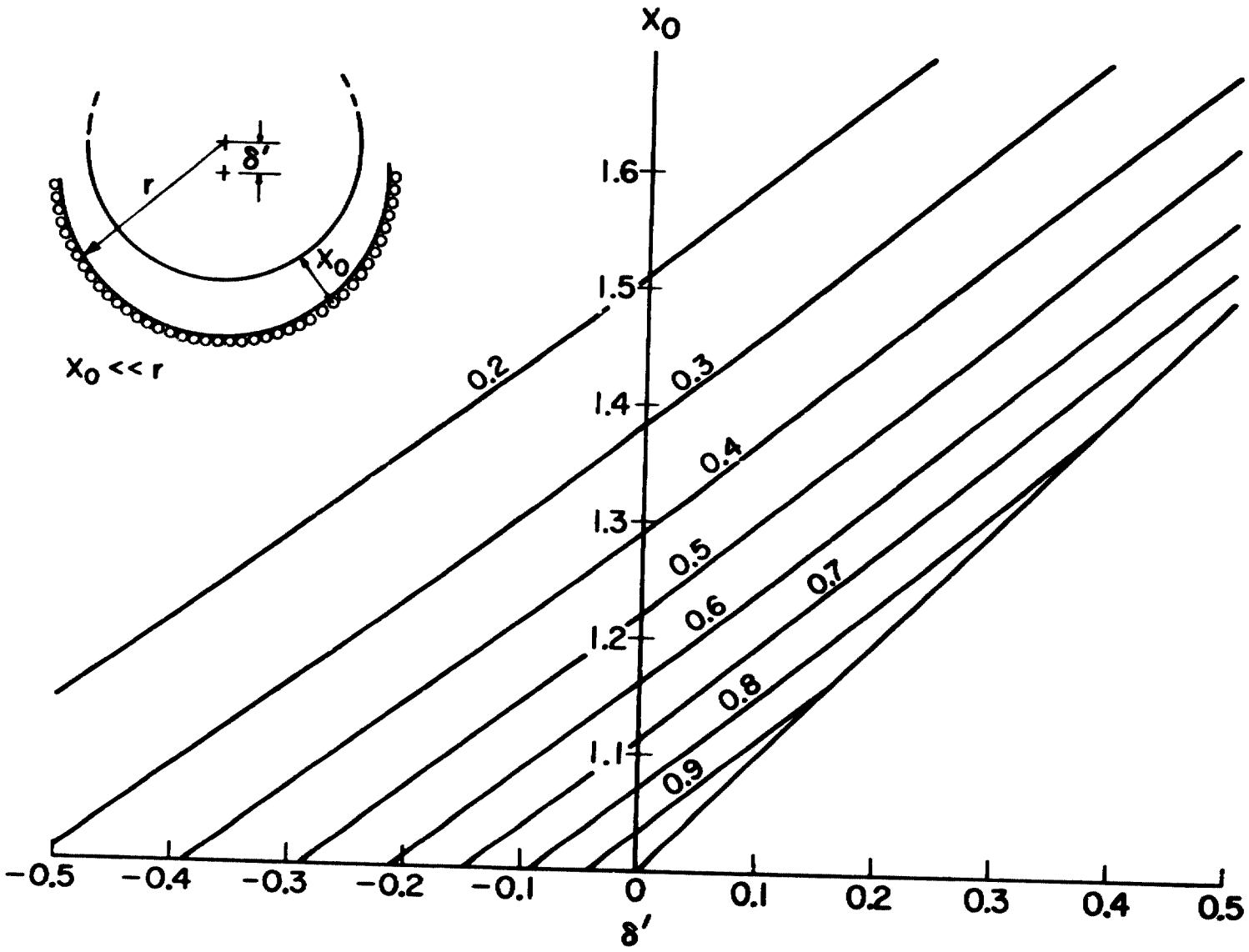

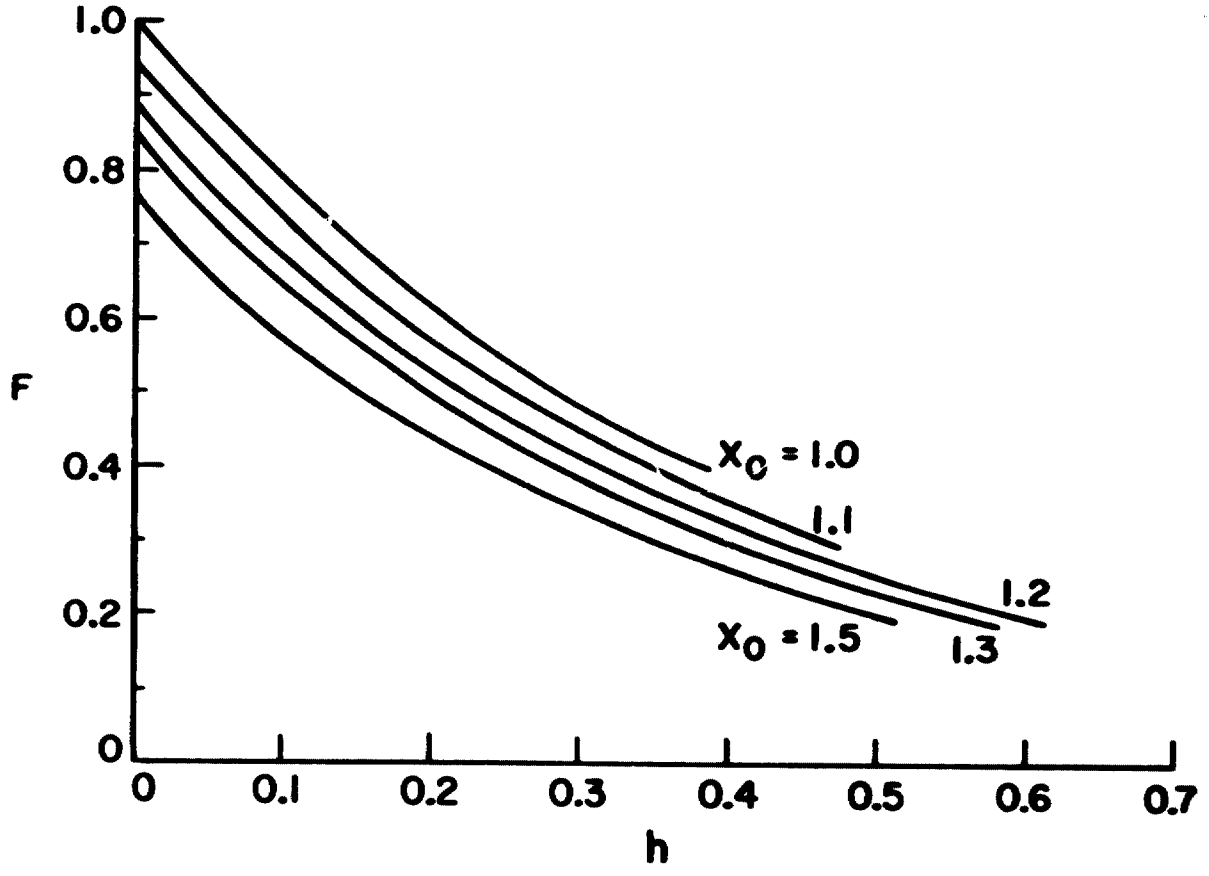

Figure 7B

Fraction of Total Force as a function of normalized height h

depends largely on the array of wires not being an infinite plane.

The total torque on the mass tilted by an angle ψ in the vertical plane is

$$\tau = \int_{-\ell}^{\ell} \tau(x)dx = \int_{\ell}^{\ell} x \left(\frac{\pi I^2}{2c^2s^2}\right) e^{-\frac{\pi(x\sin\psi + h_o)}{s}} dx \quad \text{where } 2\ell \text{ is the}$$

length of the mass and x is the horizontal distance along it. For small ψ this evaluates to

$$\tau = \frac{\pi I^2}{2c^2s^2} \cdot e^{\frac{-\pi h_o}{s}} \cdot \frac{2}{3}\ell^3 \frac{\pi}{s}\psi \quad , \text{ where we have used the previous}$$

definition of equilibrium height. The resonant frequency in ψ is thus

$$f = \frac{\omega_o}{2\pi} = \left(\frac{-d\tau/d\psi}{J}\right)^{\frac{1}{2}} = \left(\frac{2\pi mg\ell^3}{3JSA}\right)^{\frac{1}{2}}, \quad \text{where J is the moment of inertia.}$$

One further simplification can be made: $J = m\alpha\ell^2$ where α is some function of the geometry of the mass. With this,

$$f = \left(\frac{2\pi g\ell}{3\alpha As}\right)^{\frac{1}{2}} \qquad [12]$$

In this approximation the frequency depends only on geometrical properties of the mass and bearing and on the gravitational field.

The above conclusions on resonant frequencies are true only when the mass is forced down by its own weight and not when it is confined from above by another section of bearing. As an example of another situation, consider a mass sandwiched between two infinite plane arrays similar to those considered above. The total force is

$$F = \frac{A\pi I^2}{2c^2s^2}\left(e^{-(\pi/s)(\ell+h)} - e^{-(\pi/s)(\ell-h)}\right) = \frac{A\pi I^2}{4c^2s^2} e^{-\frac{\pi\ell}{s}} \sinh\left(\frac{\pi h}{s}\right),$$

where ℓ is the clearance.

The resonant frequency is found from

$$\omega_o^2 = -\frac{1}{M}\frac{dF}{dh} = \frac{AI^2}{c}\frac{\pi^2}{s^3}e^{\left(-\frac{\pi\ell}{s}\right)}\cosh\left(\frac{\pi h}{s}\right) . \qquad [13]$$

This is relatively independent of h (at least near h = 0, the center of the bearing), but is rather sensitive to the clearance.

c) Losses

Losses in the bearings are due to three main effects. These are gas damping, eddy-current damping, and losses in the superconductor. The high frequency vibrational modes may also couple to mechanical vibrations in the test mass and cradle leading to losses which are not calculable without detailed information on the system.

Losses in the superconductors themselves are for the most part negligible compared to the other two sources.[4] If any normal metal is present it may contribute significant amounts of damping. The first inner bearing (1 cm diameter) was made with copper jacketed niobium-titanium wire which reduced the Q of the longitudinal mode to less than 50. The model for this case is a distributed resistance in parallel with the ideal inductance of the magnetic bearing: any length of wire of inductance L has a proportional resistance $R = \gamma L$ in parallel with it. The resultant time constant $L/R = \frac{1}{\gamma}$ characterizes a change in flux due to the mass motions: The power dissipated by a motion ϕ at angular frequency ω is $\frac{\phi^2 R}{(1+\omega^2/\gamma^2)}$ per unit length. Any losses are detrimental to the equivalence principle experiment, and we have therefore eliminated the copper jacket in the newest 5 cm bearing. For a detailed analysis of eddy-current losses in copper-jacketed superconductors, see Ref. 2, Appendix II, and Ref. 5.

4 P. Penczynski, H. Hentzelt, G. Eger, "Measurement of the temperature dependence of the 50 Hz alternating current losses of superconducting stabilized niobium conductors" Cryogenics, Vol. 14 #9, p. 503-8, Sept., 1974.

5 Paik, H., Analysis and development of a very sensitive low temperature gravitational radiation detector. (Stanford Univ., Ph.D. Thesis, 1974).

Gas damping is significant for any but very small pressures. The damping is due to momentum transfer by gas molecules between two surfaces; roughly speaking, at low pressure the momentum transfer per unit time is

$$\Delta p = \frac{n}{2d}\sqrt{mKT}\ V = \eta V$$

where n is the number density of molecules, m is their mass, d is the separation of the surfaces, V is the velocity of one surface, K is Boltzmann's constant and T the temperature. The damping constant η is thus about 10^{-4} gm/sec at 1 mm pressure for He gas, and proportionally smaller at lower pressure. For a 50 gm mass the damping time from this source alone (at 1 mm pressure) is about 200 seconds.

IV. CONSTRUCTION OF THE BEARINGS

The construction of magnetic bearings to the design given above is a complicated task. The small scale height of the magnetic field requires close tolerances on the positions of the wires, and the straightness requirement adds to this. Because experimental performance is directly related to the performance of the bearing we set the design tolerance at about 3×10^{-4} cm, the limit of easily available machining techniques.

Several versions of the levitation cradle assembly were completed prior to the receipt of this contract. They ranged from catastrophe to moderate success. Under this contract we have perfected the design and completed a second generation instrument which meets many of the requirements. We have also designed a third generation levitation cradle which solves the remaining known problems; its construction has been delayed mostly by non-availability of a suitably nonmagnetic filler material.

i) methods

As previously discussed, the design goals for the tolerances on the positions of the wires are extremely high. The only way that they can be approached is to initially position the wires on a preform (made from aluminum), check their positions as nearly as possible, and then cast them in place with an expansion-matched epoxy. The preform is then removed by etching it out with sodium hydroxide solution, leaving the wires of the cradle on the inside of a hollow half cylinder. Small modifications to the technique could as easily produce a full cylinder.

Figure 8 is an outline drawing of a preform for the inner levitation cradle. Seventy-two grooves are equally spaced around half of the aluminum cylinder. The grooves are "V" shaped with a 90° corner pointing radially inwards and are $0.0127 \pm .0003$ cm. deep. The maximum allowable taper of the form is 3×10^{-4} cm. Past the ends of the grooved section are sets of #80 holes drilled radially into the preform. These holes are spaced in the ratio

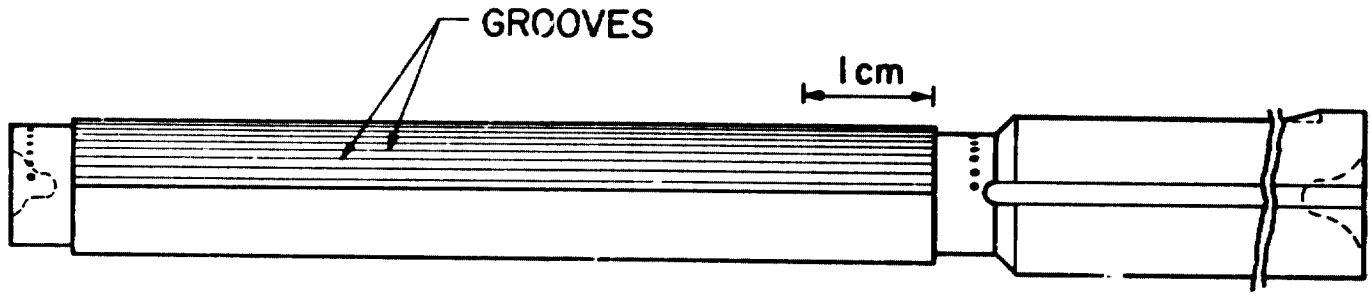

COIL FORM (SIDE)

(a)

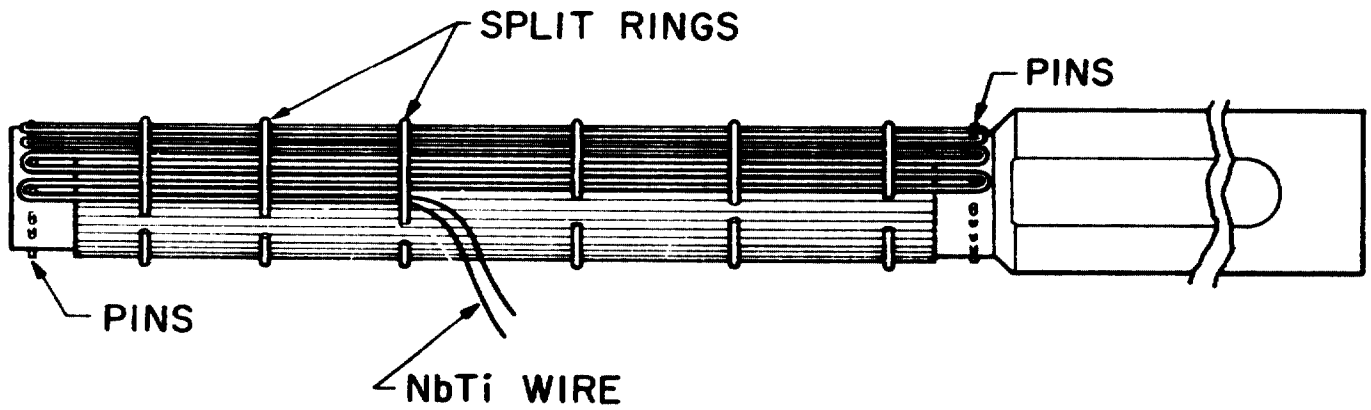

COIL WINDING (TOP)

(b)

Figure 8

of one for every four grooves, except near the ends of the coil, and hold stiff pins of phosphor bronze wire. One end of the preform is enlarged and positions the coil during casting.

The preform is made so that it requires minimum etching time to remove it. The best technique is to prepare a thin shell of aluminum of slightly smaller inside diameter than the outside of a cylindrical aluminum plug. The plug is inserted in the shell by cooling the plug in nitrogen while heating the shell to just under the annealing temperature and making a shrink fit. For purposes of machining this assembly can be treated as one piece. By slitting the shell, the central plug containing most of the material can be easily removed.

Winding the magnetic bearing begins with a long piece of superconducting wire that is doubled back on itself. It is helpful to color half of the wire starting from the bend. The bend where the wire is doubled is looped around the last phosphor bronze pin on the preform, and the pair of wires preceeding from this beginning is laid into the grooves opposite the pin. A set of split rings of phosphor bronze of the same inside diameter as the outside of the preform serve to hold the wires in the groove; they are pushed around to best hold the wires. At the opposite end of the preform the pair of wires is bent around the pin found there in a manner that guarantees that wires in adjacent grooves will carry current in opposite directions, and laid in the grooves going the other way (Figure 8b). This process is repeated until all the grooves are filled. The bronze pins are then bent away from the center of the preform to put tension in the wires; finally a phosphor bronze spring is wound tightly around the entire assembly as the split ring clips are cut off. This ensures that wires are properly in place in the grooves. After cleaning, the coil is inspected at various magnifications under a microscope, and if no serious imperfections are discovered it is judged ready for casting.

Figure 9 shows a portion of the surface of the current outer bearing before casting. The vertical bars are the bronze spring that holds the superconducting wire in the grooves. The one hundred and eighty wires are on 0.044 cm centers and are about 0.025 cm in diameter. The finished bearing has an inside diameter of 5 cm.

The support structure, which together with the magnetic bearing forms the levitation cradle, has until the present been made from a monolithic copper block. This provided strength enough to resist thermal stresses and is inert enough to resist the etching solution that removes the aluminum preform. For the third generation levitation cradles we are abandoning this brute force approach and using an expansion-matched quartz-filled epoxy, which will eliminate the thermal stresses and be chemically inert as well. The principal problems with this will be uniformity of curing and finding a sufficiently pure quartz filler.

The copper support structure is prepared by sandblasting the concave surface only, and then carefully cleaning the roughened surface in an ultrasonic cleaner, with a very light acid etch if the surface seems extra dirty. Although the filled epoxy is a good match to the thermal expansion of copper, this sort of surface preparation was found necessary to insure that the thin (~1 mm) layer of epoxy would not pull up from the support cradle, especially in the case of the outer cradle. Thermal cycling of a large area of thin epoxy on a smooth copper surface usually removes it quickly unless special care is taken; the different heat capacities and thermal conductivities of the materials allow them to cool at different rates, with the result that a layer of epoxy may have a temperature difference from one side to the other of one or two hundred degrees. The resulting thermal stress can easily break a poor bond. Most thermal cycling problems will be eliminated in the third generation design.

Figure 9

Detail of Surface of Outer Bearing

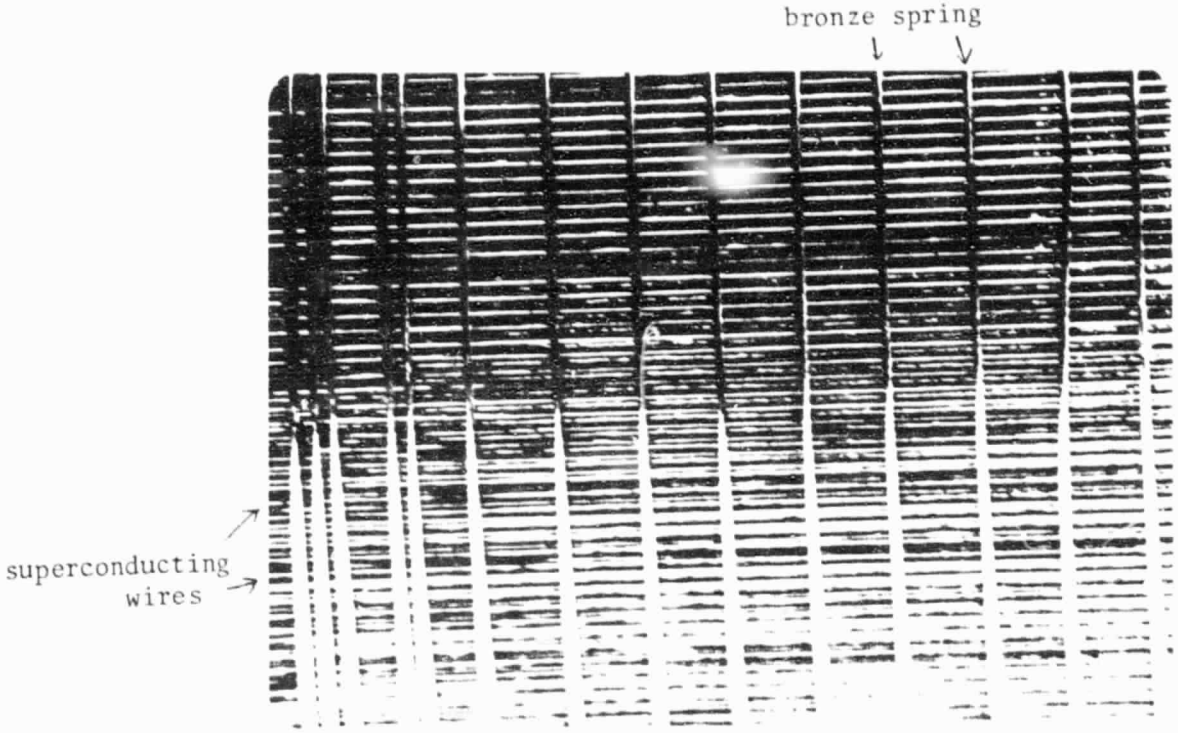

The levitation coil and the interior of the support cradle are painted with catalyzed epoxy using a Q-tip; they are then fitted together and clamped in place. A short period of vacuum outgassing removes any macroscopic bubbles and usually causes the epoxy to foam out over the edges of the support cradle. This material is removed while still fluid; the space between the coil and support cradle is refilled with previously outgassed epoxy. After curing the levitation cradle is ready for removing the preform.

The etching process requires some care because the bond strength of the epoxy is decreased by prolonged exposure to sodium hydroxide; furthermore, the material softens somewhat during etching because of the heat. First the core of the preform is removed to shorten the etching time, or alternatively the center is milled out to within about 1 mm from the surface of the coil. The entire levitation cradle is then placed in a hot concentrated solution of sodium hydroxide and the aluminum is etched out as rapidly as possible, to minimize diffusion of NaOH into the epoxy. The etching can usually be stopped early because the aluminum becomes undercut and releases from the coil. The levitation cradle is then inspected and touched up with #600 sandpaper and a scalpel to remove excess epoxy.

A final stage is necessary to finish the bearing. This consists in polishing the interior surface of the wires with a mockup of the test mass coated with very fine abrasive powder, to remove more excess epoxy and make the surface more uniform. The smoothness of the surface then depends less on the precise placement of individual wires.

ii) Measurements on cradles

This process produced levitation cradles almost as accurate as the design goal of $\pm$ 3 x 10^{-4} cm. Figure 10A shows the measured horizontal diameter of the second outer levitation cradle produced without the final polishing. The average diameter was 5.0297 $\pm$ .0013 cm overall; in the central region -- leaving out 2 cm. near each end -- the diameter was 5.0302 $\pm$ .0005 cm. The equivalent $\frac{d^2h}{dx^2}$ was about 10^{-4} -- close enough to be touched up by the polishing process. This bearing was damaged during manufacture and we were unable to salvage it.

Radial positions of the wires are important to prevent large variations in the normal force. Figure 10B shows the measured radial variation of the same cradle. The RMS variation from a perfect cylinder was overall about 7 x 10^{-4} cm.

In order to save effort we decreased the number of wires in the present outer cradle to 180 from 360. Unfortunately, due to insulation which softened in the epoxy, this bearing had a worse deviation of about 11 x 10^{-4} cm. By the polishing process we have improved this to the point where the bearing is probably usable.

The critical thing for the bearings is not their physical shape but the shape of the force they produce. We used two techniques to measure this. The most sensitive method is usable only if the mass has stable positions within the bearing. Measurement of the period is equivalent to measurement of $\left(g\frac{dh^2}{dx^2}\right)^{\frac{1}{2}}$. In fig. 11, $\frac{d^2h}{dx^2}$ or ω^2 is plotted as a function of magnetometer position for the first inner levitation cradle we produced. The periods are all very much shorter than expected from measurements of the shape of the cradle. On the basis of independent measurements of susceptibility we blame the epoxy used to hold the bearing together: it is badly contaminated with tiny particles

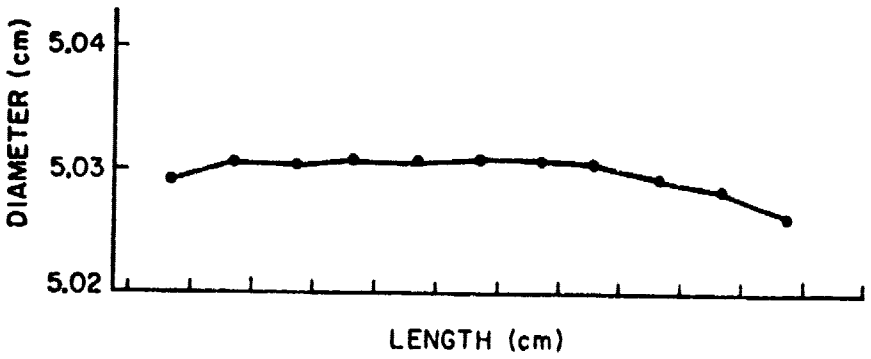

Figure 10A

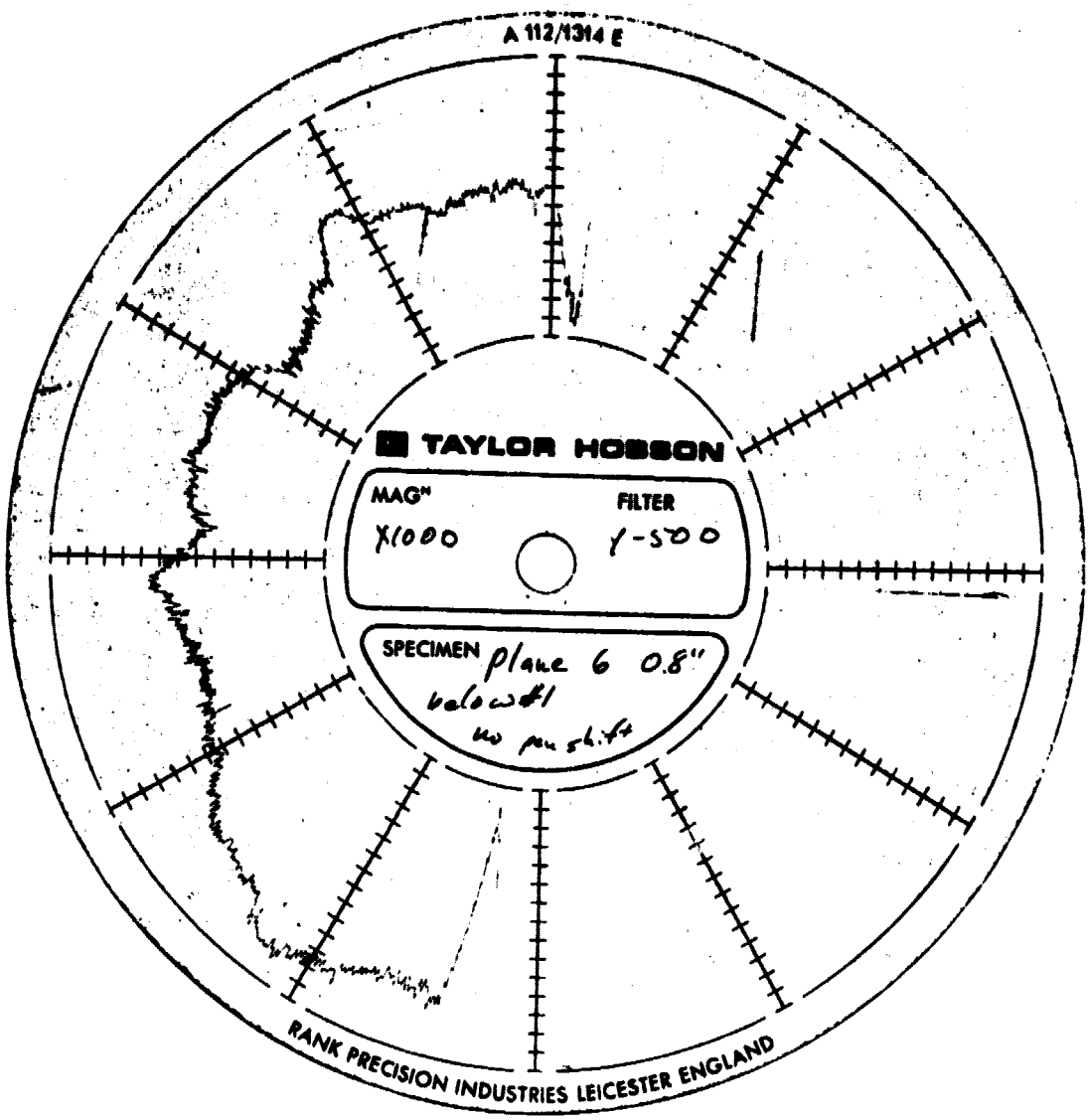

Typical Radial variation of
outer levitation cradle
before finishing

Figure 10B

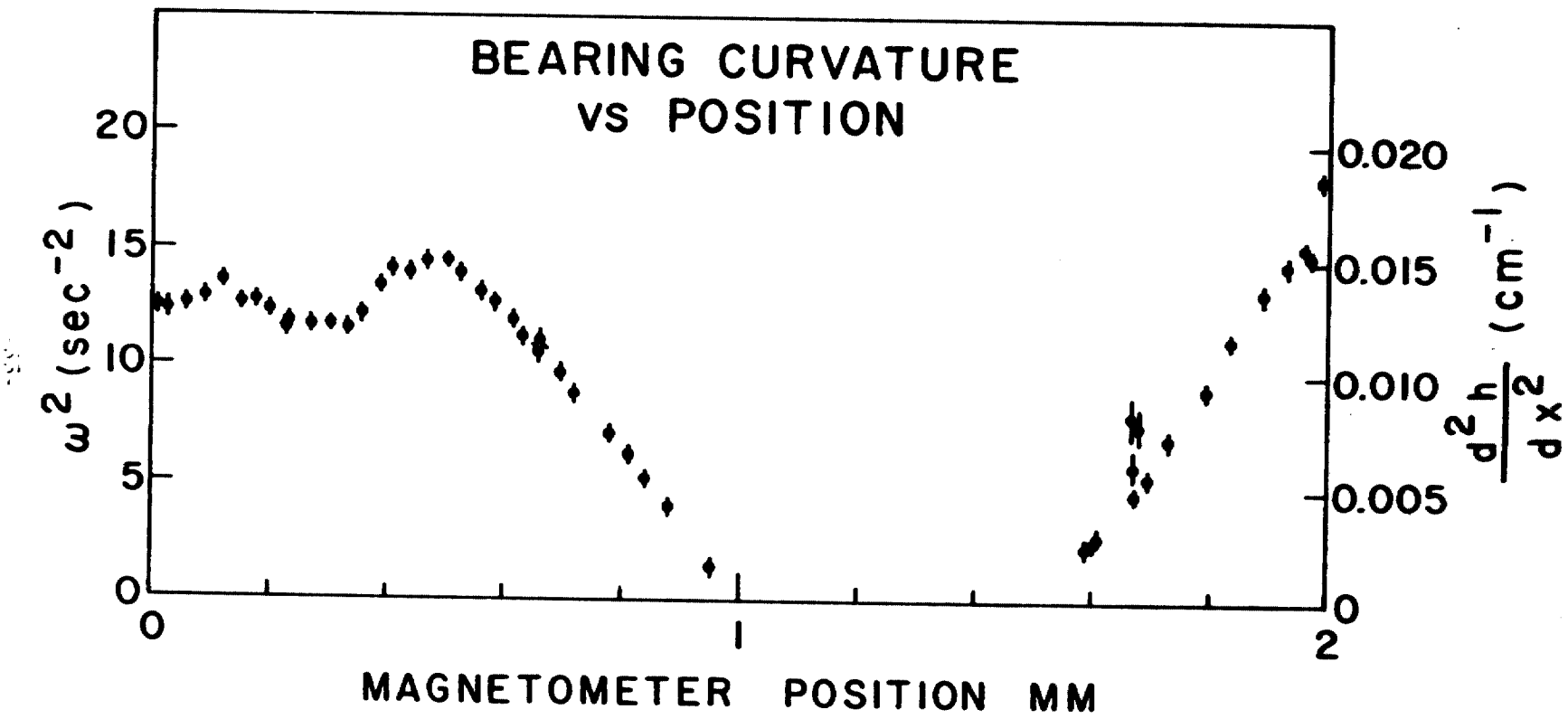
BEARING CURVATURE
VS POSITION
20
15
10
5
0
ω^2 (sec^{-2})
0.020
0.015
0.010
0.005
0
$\frac{d^2h}{dx^2}$ (cm^{-1})
0
1
2
MAGNETOMETER POSITION MM

Figure 11

of iron, which become strongly magnetized and cause lumps in the magnetic field. Only small regions of this bearing could be used for the equivalence principle experiment.

The second method is direct measurement of the acceleration of the test mass as it slides back and forth in the bearing. An initial estimate for $\frac{d^2h}{dx^2}$ is found from the angle required to start the mass sliding. The dewar must be tipped through at least 24×10^{-5} radians to cause the outer mass to slide from one end to the other and back. This measures the curvature since $\Delta\theta \approx \left(\frac{d^2h}{dx^2}\right) \Delta x$, so that $\frac{d^2h}{dx^2} \sim 12 \times 10^{-4}$ cm^{-1}. This estimate can be regarded only as an upper bound since a slight tendency to stick to either end (for example if the mass is electrically charged) could equally well explain the result.

By measuring the acceleration of the mass as a function of position for several slides at different angles we can derive a plot analogous to figure 11. The result is relatively much noisier than period measurement, because of the short time of measurement and superposition of seismic noise. Furthermore, it is not independent of the position detector: it is impossible to tell with a single slide whether the measured acceleration is real or due to some nonlinearity of the measurement. With several slides we can make a separation.

If the measured position is M(x) where x is the real position, then $\ddot{M}(t) = \ddot{x}(t)\left(dM(x)/dx\right) + (\dot{x}(t))^2\left(\frac{d^2M(x)}{dx^2}\right)$ where dM/dx and d^2M/dx^2 are unknown functions of the position detector and $\ddot{x}$ and $\dot{x}$ are the real acceleration and velocity. Since $\dot{M}(t) = \dot{x}(t)\left(dM(x)/dx\right)$ we can eliminate $\dot{x}$. $\dot{M}$ and $\ddot{M}$ are found from the original measurement M, so for each slide we have an independent equation of the form

$$\ddot{M}\left(\frac{1}{dM/dx}\right) - \dot{M}^2\left(\frac{d^2M/dx^2}{(dM/dx)^3}\right) - \ddot{x} = 0$$

at each point x. Finally we note that $\ddot{x} = g(\theta + dh/dx)$ where h is the height function of section III. i that measures the straightness of the bearing. We

measured M(t) and θ for a number of slides usin the capacitance meter, and calculated $\dot{M}$ and $\ddot{M}$ for 25 positions along the bearing, and solved for $\frac{1}{(dM/dx)}$, $(d^2M/dx^2)/_{(dM/dx)^3}$, and dh/dx at each position for different groups of three slides.

The resulting measurement of dh/dx is shown in figure 12. The prints are solutions for the "best" three slides, i.e., those which showed the least seismic noise. The crosses are for a typical set of three slides. The statistical analysis is incomplete, and there are possibly systematic errors due to the dynamic response of the dewar probe.

Taking the "best" measurement and throwing out the two anomalous points, we can say that dh/dx is everywhere about -2 ± 17. Consequently over the 2 mm range of motion d^2h/dx^2 is less than 9×10^{-5}. Even the noisy measurement implies d^2h/dx^2 is less than about 1×10^{-3} -- more than an order of magnitude better than the contaminated inner bearing. These numbers represent the limit of measurement rather than any actual value for d^2h/dx^2.

We were able to measure the height of the test mass as a function of trapped current for the outer bearing by using the capacitance height detector. This measurement was complicated by nonlinearities from the curved capacitor plates and to a lesser extent from the core of the flux transformer. The capacitor plates could be calculated pretty exactly but the transformer needed an empirical model fit to some earlier data. Finally there was a matter of scale factor: we have never been able to accurately calibrate the secondary current of the transformer for lack of a suitable instrument that works at $4^{\circ}K$.

FIGURE 12

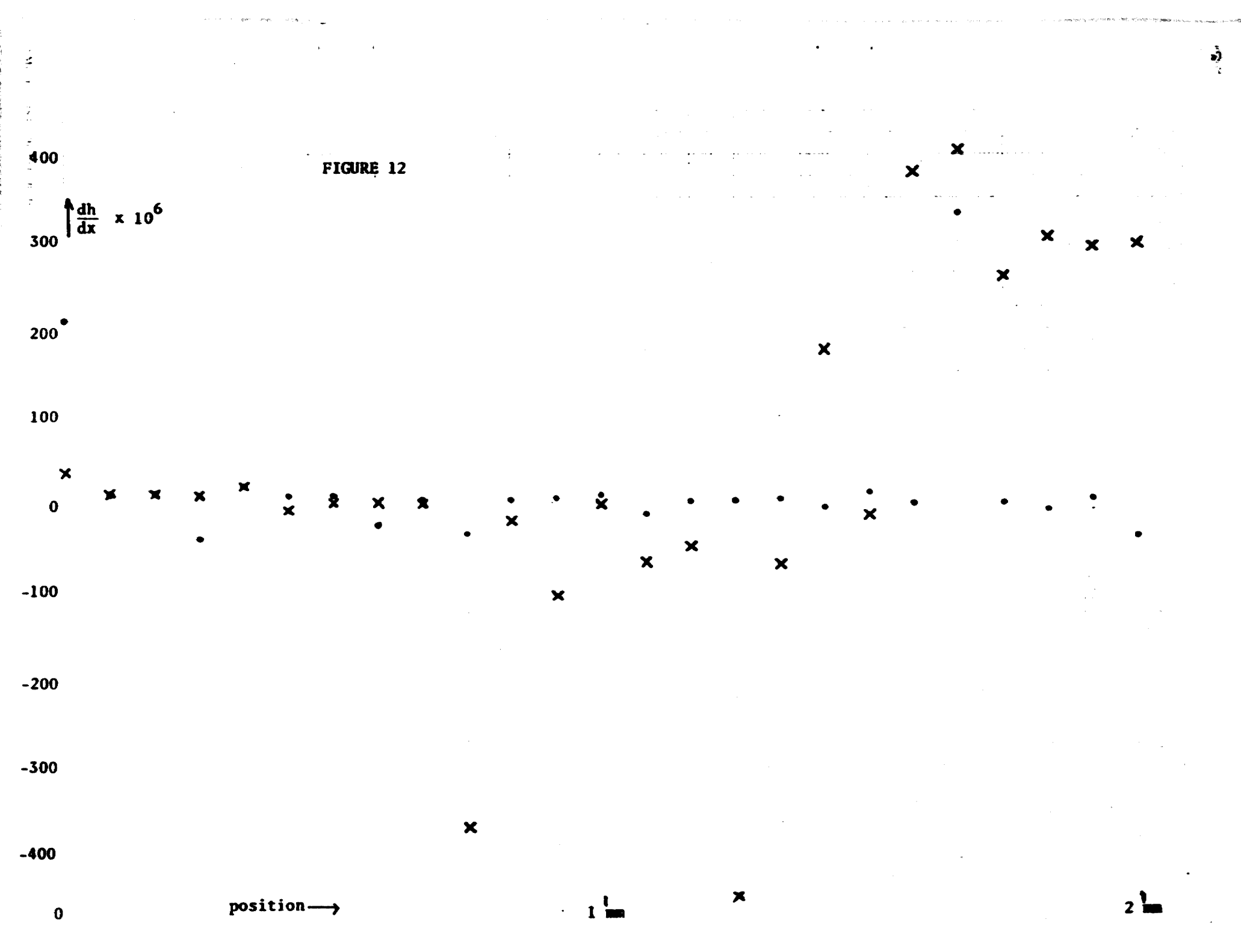
400
300
200
100
0
-100
-200
-300
-400
$\frac{dh}{dx} \times 10^6$
0
position ⟶
1 mm
2 mm

The resulting fit is shown in figure 13; in the theoretical curves only the initial slope was matched. The electrical contact in this series of measurements was due to one of the wires of the bearing buckling outward under thermal stress and contacting the test mass. The theoretical fit was calculated using equation (10).

We have also measured the principal resonant frequencies of the bearings; the results are in good agreement with eqns. (11) & (12). Figure 14A shows several resonances of the inner bearing. For this the mass was observed with the SQUID magnetometer position detector, at several heights as determined by the current in the primary of the superconducting transformer. The horizontal position of the mass was not determined. The mass was excited by a 20 ma. current to the control coil beneath the magnetic bearing. The frequency of this current was swept from 10 to 100 Hz and the response amplitude measured by a lock-in detector. Three points must be made to clarify fig. 14A (and 14C as well): 1) the control coils do not uniformly excite all the modes. The vertical and tilt modes are preferentially excited, but the amount depends on the persistent current in the control coil loop. The other modes are excited only indirectly. 2) the SQUID position detector circuit is directly sensitive only to longitudinal motions of the test mass. It is sensitive to all of these motions only in second order, as required for the equivalence principle experiment. 3) because of instrumental limitations it was necessary to sweep the frequency at a high rate and use a wide bandwidth. Consequently most of the signal is due to excitation by seismic noise,

which accounts for the variability in line shapes. This is adequate for low-resolution studies of the resonant frequencies. Figure 14B shows the response of the inner mass around 58 Hz with a 100 second time constant and suitably slow sweep rate, which effectively removes the seismic response. Figure 14C shows measurements equivalent to 14A but for the outer test mass.

The modes were identified by association with the calculated value or by their response to experimental parameters. The vertical and pitch modes show particularly good agreement with values predicted from equations (11) & (12) which they approach as the masses are levitated higher and higher. The other modes cannot be calculated so precisely because they depend critically on the clearance between the mass and bearing, which is very hard to determine accurately.

Since we acquired a microcomputer data recording system early this year we now have the capability of performing these frequency measurements more quickly. Figure 15 is a fast fourier transform of the signal from the outer test mass just after it was excited by bouncing against the end of the cradle. A 66 Hz resonance (probably vertical mode) was particularly excited.

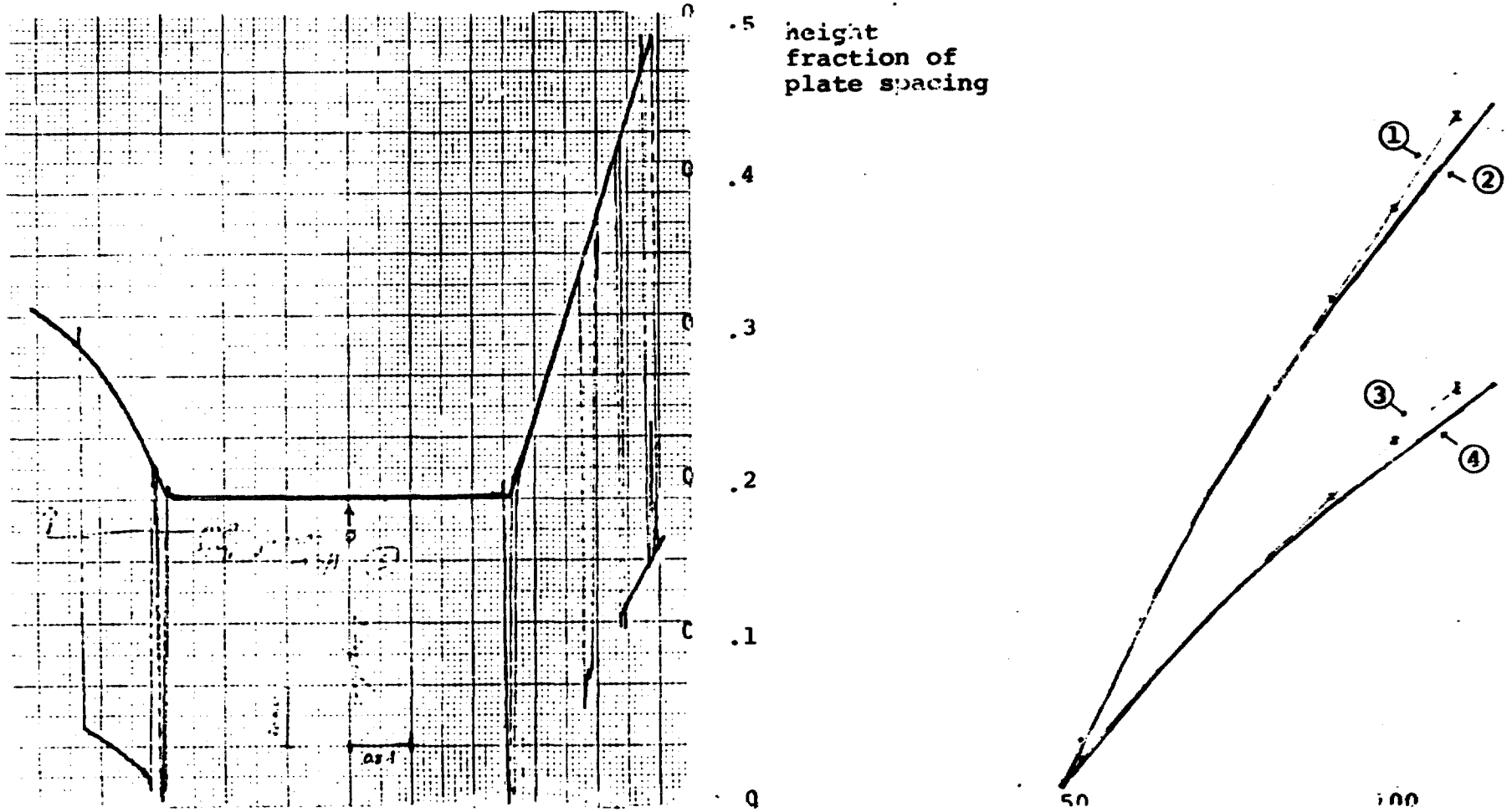

Left - Raw Data
Figure 13 - Right - Data adjusted for nonlinearity in height and current (arbitrary units)

Curves 1 and 3 - data
Curves 2 and 4 - theory
Curves 1 and 2 - mass making electrical contact to cradle
Curves 3 and 4 - mass not contacting cradle

Figure 14

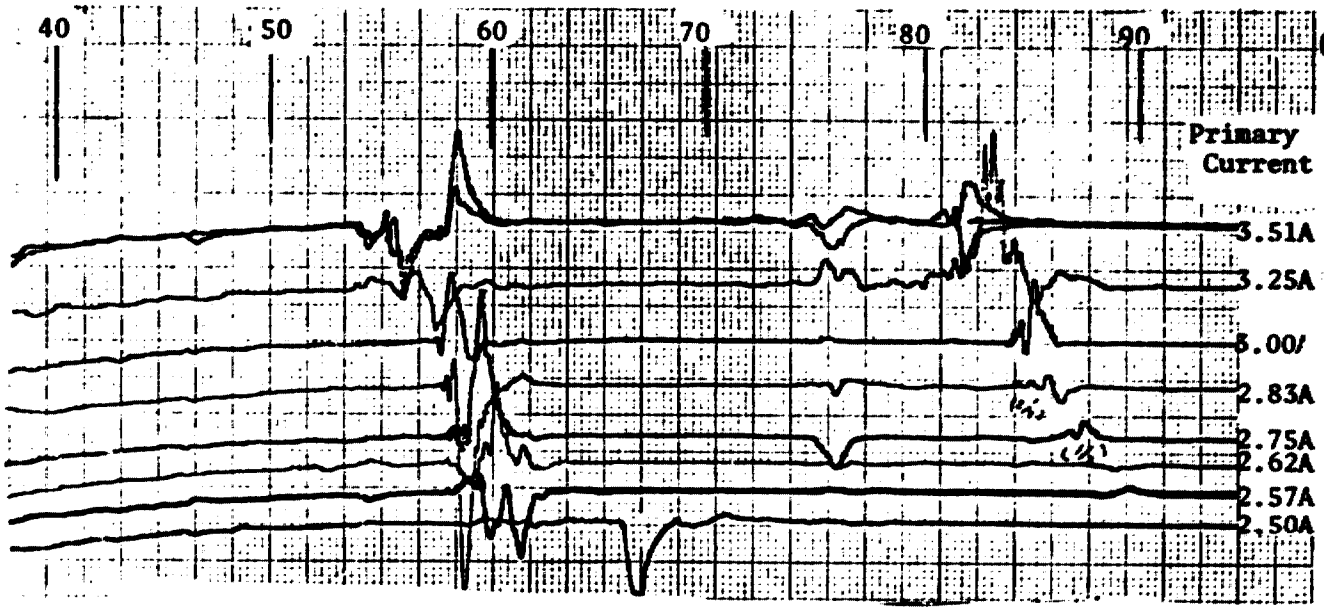

(A) High Frequency modes of Inner-Test mass excited by control coils

84 Hz - Vertical Mode
58 Hz - Pitch Mode
75 Hz - sideways mode or yaw mode

(B) 'Real' line shape of 58 Hz mode

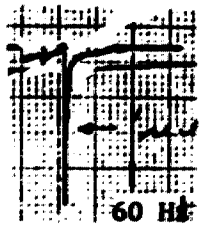

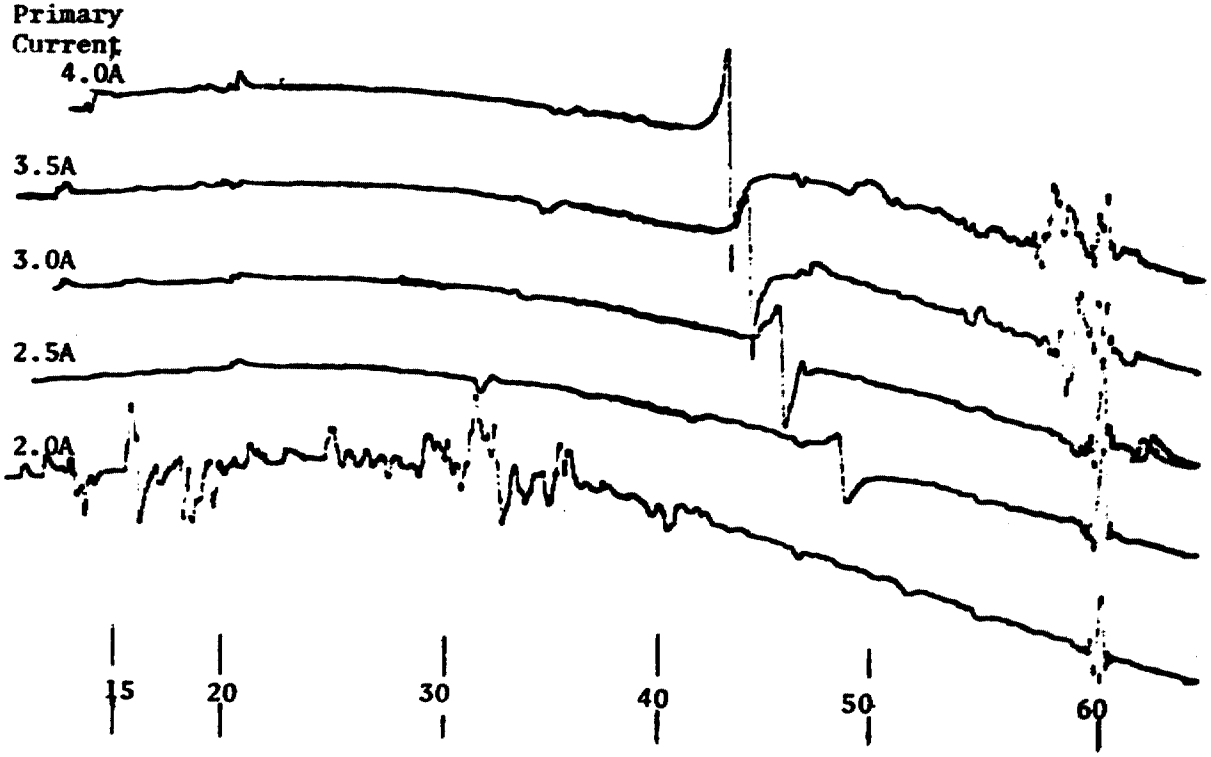

(C) High frequency modes of outer test mass, for different levitation currents.

59 Hz - vertical mode
43 Hz - pitch mode
35 Hz - yaw mode

Figure 15.

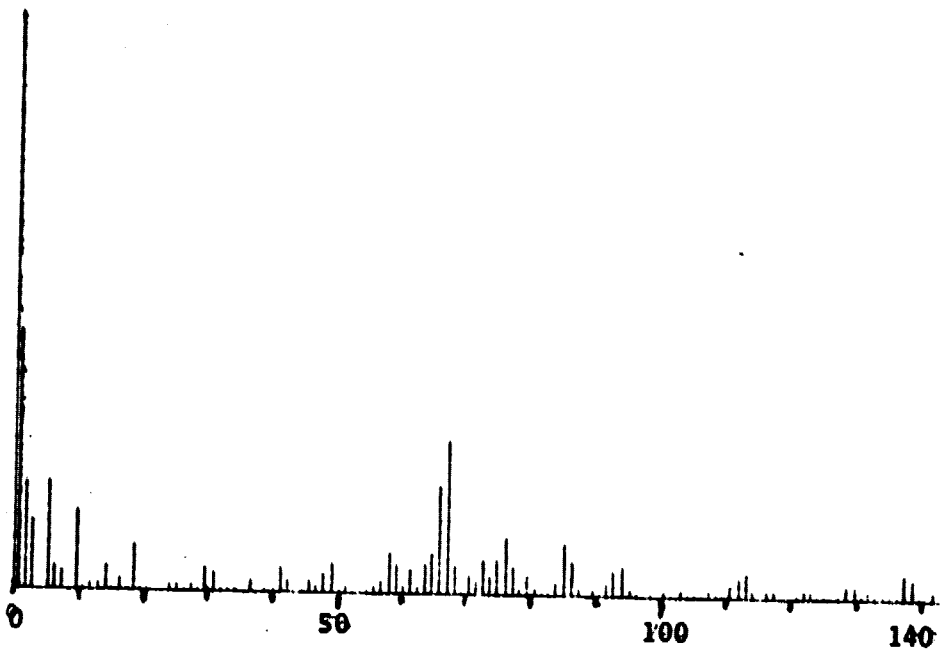

Outer Test Mass Frequency Spectrum

V. ANCILLARY MEASUREMENTS

i) Position Detector

The position detector circuit was shown in figure 3. A general analysis is given in reference 2 , which demonstrates the characteristics of the detector without exact computation. We now have the ability in principle to measure the response of the position detector and compare it with numerical calculations, but a quantitative measurement has been delayed by several factors. One of these factors is related to the position detectors. The magnetometers are somewhat more likely to lose lock than we expected (actually for calibration purposes we are expecting them to handle higher rates of charge of flux than we originally intended), so that we found it very desirable to put a 100 microhm short across the SQUID input. This reduced the response to seismic noise above 10 Hz and reduced the load on the magnetometer. This puts an approximately 0.1 second delay into the signal, which is negligible for static measurements but significant for one method we intended to use to calibrate the detector. Neither the unlocking or the time lag will be significant at the much smaller signal levels of the equivalence principle experiment.

The qualitative agreement of the position detector with theory is excellent. We have been able to show that the sensitivity is within a factor of five of theory: this is about the range expected since the theoretical sensitivity varies with position. We can demonstrate that the sensitivity changes linearly with trapped current and also increases as the mass nears either pickup coil. The detector for the inner test mass behaves exactly like the theoretical model, and we have recently confirmed that some anomalous behavior of the outer detector is explained by the same model with either a heat switch failure or an equivalent wiring error.

The most accurate method of calibration we have is to tilt the dewar a measured amount θ while the test mass is in a stable potential well with known period. The force constant is determined by the period and mass, so the displacement can be calculated from $x = \frac{g\theta}{m\omega^2}$. The method is time-consuming and we have done only a few points by hand. Figure (16) shows the results at one position for different trapped currents in the inner position detector. We have not had time to repeat this measurement with the new computer data system but we expect it will be much quicker and easier. This method has the serious disadvantage that it works only if the mass has a stable position, which is less likely if the bearing is approaching the desired smoothness.

The other method of calibration is to slide the test mass from one end of the bearing to the other. Since the force is either small or known from independent measurements (see p. 31ff) the magnetometer output M(x) could be found from a single slide. Because of the time delay this method gives only qualitatively correct results; furthermore the magnetometer still loses lock when the mass moves too rapidly. Although both the time lag and unlocking are well determined, it is computationally infeasible to deconvolve the magnetometer output to get quantitative agreement with theory.

We are beginning work on the position controller for the test masses, which will artificially give the test mass a period determined by the experimenter. With this it will be possible to automate measurements of the first method and complete the calibration.

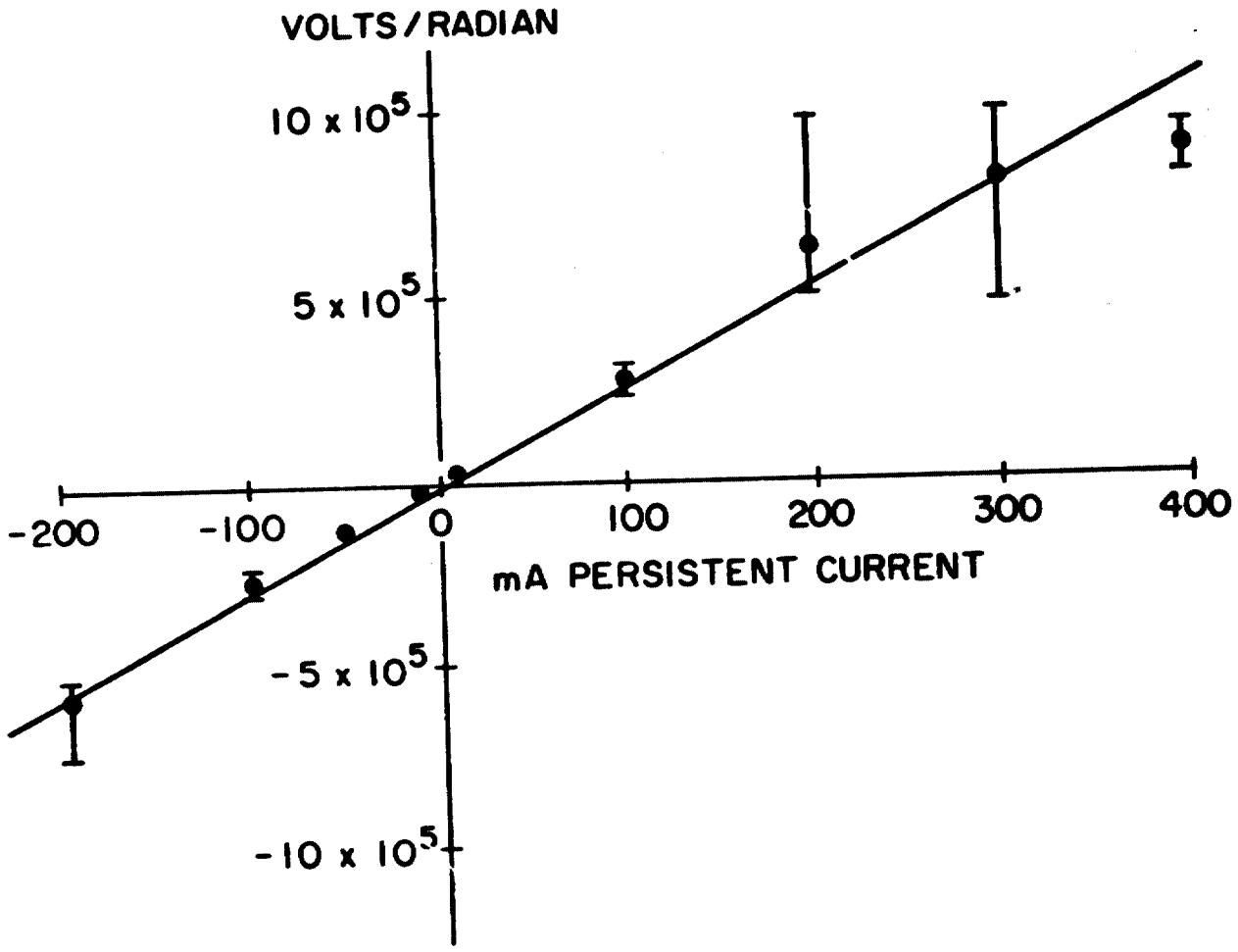

CALIBRATION OF INNER POSITION DETECTOR

Figure 16

ii) Preparation of the Masses

One of our early results was that preparation of the test masses is very important if they are expected to float on a magnetic field. Levitation of a type I superconductor depends on its critical field, which determines the largest magnetic pressure that can be expected against it. The equivalence principle experiment should use type I superconductors because they have less tendency to include trapped flux when they become superconducting.

If the critical field H_o of a superconductor is too low, an object made of it cannot be levitated in a gravitational field g. The problem is complicated because the effective critical field depends on the geometry of the superconductor as does the total force. As an approximation we assumed the mass of superconductor to be cubical with side S and a magnetic field $H_\parallel$ applied to the lower face. The criterion that the mass should lift is

$$\frac{H_\parallel^{\,2} S^2}{2\pi} = mg$$

where $m = \rho S^3$ is the mass of the cube and ρ is the density. For a given material we can derive from this a figure of merit

$$\psi = \frac{H_o^{\,2}}{\rho} = 2\pi Sg$$

which relates the critical field and density to the largest cube that can be lifted in the gravitational field; for a 1 cm cube ψ must be greater than 6157 $(\frac{cm^2}{sec^2})$. Many common superconductors exceed this value. As an example a lead cube of S = 9 cm could be supported on earth, or a 70 cm niobium cube, but not a 0.6 cm aluminum cube. Note that the critical field is dependent on temperature so that this equation is an upper limit.

If a non-superconductor is coated with a thin layer of superconductor the same treatment applies with the caveat that a thin layer may allow flux penetration.[6] With these considerations we selected solid niobium for the inner test mass and aluminum sputtered with niobium for the outer mass. The solid niobium was successful, but the niobium plated mass could not be levitated.

In fact measurements showed that the mass was levitating for brief periods (10 - 20 seconds) and then sagging back into the bearing. Tests of flux penetration showed that a strong steady field above 20 gauss tended to penetrate niobium thin films slowly over the same time scale. We suspect the cause to have been nucleation of "bubbles" of trapped flux at microscopic holes or cracks in the film, followed by spreading of the relatively mobile "bubbles" to the entire film.

On the basis of tests with a solid lead alloy test mass we prepared a new aluminum test mass with a layer of pure lead 0.002" thick electroplated onto it. Although lead has a substantially smaller figure of merit ψ than niobium we have never seen any evidence of flux penetration in the new mass. This is probably due to the relative thickness of the plating and quality of the film. This mass has levitated for periods longer than one week without sagging.

The failure of the niobium films was unexpected. We had previously levitated a test piece of aluminum about 1½" on a side x ¼" thick which was sputtered with a 5000 Å Nb film. Sputtered Nb films are known to be sensitive to a number of factors during the deposition process.

[6] R. D. Bourke, "Flux Penetration in thin Walled Superconducting Cylinders", Stanford University, Dept. of Aero. & Astro., Sudaer No. 206 (1964).

iii) Magnet Charging Circuit

The equivalence principle experiment should operate for long periods undisturbed. Helium transfers are a major disturbance, so the probe must be designed for minimum heat leak. Currents of 50 - 60 amperes are required to drive the wire of the outer bearing normal and 15 - 25 amperes are needed for ordinary operation. Rather than suffer the enormous heat load from conductors to carry this current - or the nuisance of removable conductors - we use a superconducting transformer to charge each bearing. Only five or six amperes input is needed to drive the bearings normal.

Because the inductance of either bearing is small (~ 50 μHy) it is easy to wind a transformer primary of much larger inductance. The complicated flux pumps which must be used to charge large magnets with superconducting transformers [7] are unnecessary. The solution of the persistent current transformer is exactly analogous to a normal transformer. If the primary and secondary inductances are P and S and have mutual inductance M, the current ratio for a load inductance L is $\frac{I_S}{I_P} = \frac{M}{L+S}$. The difference from an ordinary transformer is that the secondary current I_S is superimposed on a pre-existing supercurrent I_T which may be changed by making part of the secondary loop normal briefly with an appropriate current in the primary.

After initial experimentation with air core transformers (which were too bulky) we wound toroidal transformers on tape wound cores (ferrite cores usually have a much smaller permeability at 4^{o}K than at room temperature) with approximately 10:1 turns ratio, and with secondary inductances matched to their respective magnetic bearings. The major difference in operation from an ordinary AC transformer is magnetization of the core. As long as the secondary circuit is superconducting the flux in it is constant and the magnetization does not change state. If the critical current of the secondary

[7] Bernard, S. P., Atherton, D. L., Rev. Sci. inst. Vol. 48 #10, p. 1245-49, Oct. 1977; p. 1250-52, Oct. 1977.

is exceeded the secondary becomes normal and permits the flux to change; the core becomes highly magnetized and has a lower effective permeability until a reversed current pulls it out of saturation. The resulting transfer function (fig. 17) has a characteristic shape.

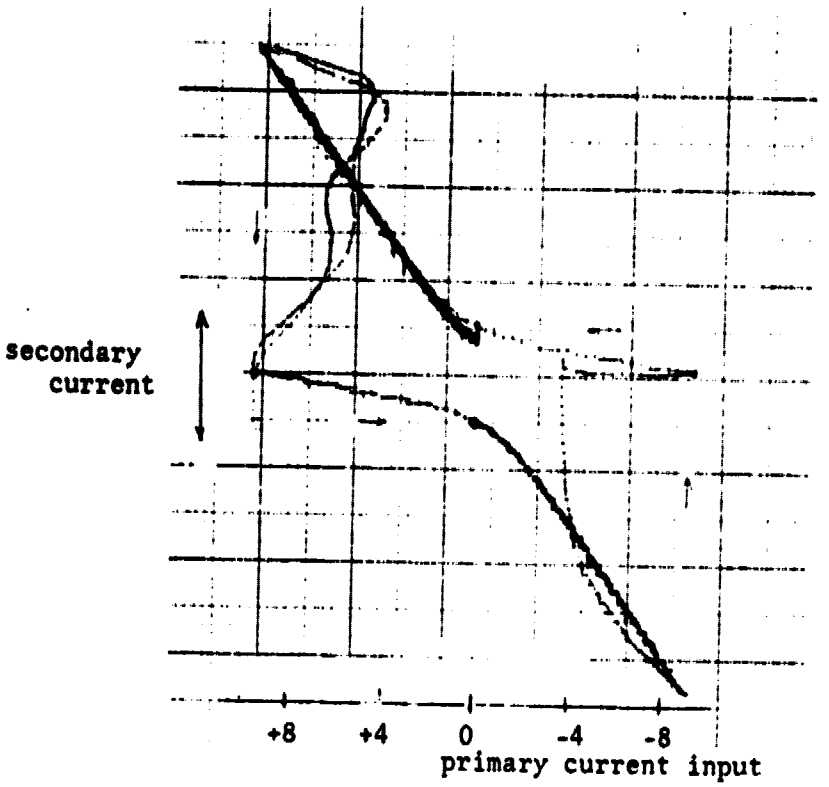

Figure 17

Flux transformer DC current transfer. The critical current of the secondary was approximately 50 amperes. Superconducting to normal transitions occurred at about ± 9 amperes input.

VI. APPLICATIONS

i) General discussion

The question of superconducting bearings in spacecraft is really two questions; first that of where one might want moving parts in a spacecraft, and second, whether the need for the special properties of superconducting magnetic bearings justifies the additional bother and expense of using them. The second question depends on the specific application; without details we can only summarize the advantages and disadvantages of superconducting bearings. The first question is broader but permits specific applications to be discussed. We will discuss most of the applications without attention to whether the bearings are justified.

The bearing we have developed under the contract is intended specifically for the equivalence principle experiment, and is not necessarily suitable for all of the applications below, particularly for any with large variable loads. It is suitable for small to moderate loads where large stiffness and low dissipation are important, and the adaptation to other geometries is straightforward if the locally flat approximation remains valid. For example, the linear bearing is changed to a rotary bearing by winding the pair of wires helically instead of axially; the total force is given by an expression similar to (10) with the limits of integration changed. A rotary bearing would be much easier to make. A very stiff thrust bearing would be made by winding the pair spirally on the surface of a disc. A side benefit of our bearing is that it produces very small fringing fields, which may be important in some applications.

We have included an appendix on magnetic bearing types and previous research on superconducting bearings for completeness. Our bearing is type 2 in this list; type 3 is very common, and type 4 has the best potential for heavy loads.

ii) Considerations for Justification

Justification of the use of superconducting bearings is on the basis of requirements and performance. A magnetic bearing (not necessarily superconducting) has the following advantages over a mechanical bearing:

1) zero wear. There is no contact between surfaces and consequently no rubbing. As a corollary to this there are no lubricants, no bearing seizure or other failure due to normal mechanical motion.

2) inherently low dissipation. This is a further consequence of no contact between surfaces. A magnetic bearing loses energy very gradually compared to a mechanical bearing.

3) mechanical isolation. Magnetic bearings have at most six degrees of freedom, whereas any mechanical system has (for practical purposes) an infinite number. Consequently any simple mechanical system used for vibration isolation will transmit a number of unintended frequencies by mechanical or acoustic coupling. A magnetic bearing, on the other hand, can make an ideal filter because of the absence of unnecessary mode structure. Conversely, magnetic bearings are quiet and do not generate noise as do rolling or sliding surfaces.

4) thermal and electrical isolation. For some purposes it is desirable to operate a portion of an apparatus at very different temperatures or voltages; the gap in a magnetic bearing can isolate these while the bearing provides strong mechanical support.

5) adjustability. A magnetic bearing can be designed so that it is possible to adjust its separation (or any other parameter) over a relatively wide range. To do this with a mechanical bearing can be complicated. Thus a magnetic bearing can double as an actuator mechanism.

Superconducting bearings likewise have some advantages over ordinary magnetic bearings. These are:

1) Superconducting bearings are intrinsically stable. Therfore the external circuitry required is reduced to the minimum required for charging the magnet.

2) zero power consumption. If the magnets are connected in a persistent current loop they remain charged essentially forever -- i.e., until they warm up -- and require no further power input. This may be critical in spacecraft applications.

3) greater load capacity. Only superconductors can produce static fields over 100 kilogauss, which is important if very large loads are to be supported with a large gap.

4) even lower losses are possible. This requires a perfectly superconducting system, or at least the removal of normal and ferromagnetic materials to a large distance. Losses can in principle be reduced to the AC losses in superconductors, which are extremely small at low frequency.

5) reliability. Most practical ordinary magnetic bearings require external electronic circuits to operate, which can possibly fail. The reliability of a superconducting magnet, once charged, is essentially limited by the probability of its warming up. This may in some cases be smaller than the likelihood of electronic component failure.

Superconducting magnetic bearings are not without disadvantages. While they overcome certain disadvantages of ordinary magnetic bearings (such as the requirement for continuous power) some problems remain. The most important are:

1) the need for refrigeration. At present we have no superconductors that work much above 20° K. Since most spacecraft near the sun will have an

equilibrium temperature higher than that, continuous refrigeration is required. This may be by boiloff of cryogenic fluid or active heat removal. The latter requires extra power, while the former has a finite life set by exhaustion of the fluid. Consequently most applications of superconducting bearings will be where low temperature is required for some unrelated reason.

2) stiffness. Magnetic bearings cannot easily be made as stiff as purely mechanical bearings. Consequently for alignment and pointing applications or where great rigidity is required, mechanical bearings may be superior.

3) lack of losses and friction. In some applications excess vibrational motion is a disadvantage. In some magnetic bearings it is hard even to design much loss into the system, so that it must be added artificially.

4) complexity. Even the simplest magnetic bearings are complicated compared to a simple mechanical bearing.

Where the refrigeration requirement definitely rules out a superconducting bearing it is often possible to use a normal metal bearing of similar design if lesser stiffness and load capacity are allowed. By exciting the magnet with high frequency alternating current, eddy currents in normal metals produce forces which approach half of the force for the superconducting case.

iii) Potential Applications and Specific Examples

We have listed below several areas of application for superconducting magnetic bearings in spacecraft, with selected examples where these are available. Note that we have not restricted the discussion only to bearings of the bifilar type, although they are suitable for many of these applications.

1) Drag free systems. A drag free satellite uses an internal proof mass as reference to keep itself following a geodesic path. In the general case the mass is tracked in three dimensions. In the case of an earth-oriented satellite, however, most of the disturbances are from the in-track direction,

and there is a certain economy in tracking the mass only along one direction. This requires that the mass be restrained in the two perpendicular directions. This was the case for the TIP-II satellite[8] which used a tubular aluminum proof mass. The mass was repelled from a single wire threaded through the center, by induced currents from high frequency current in the wire: axial suspension forces were due only to end effects. Clearly the entire suspension could have been superconducting and powered by a persistent current. Alternatively a bearing of the type developed here could have been used, which could provide less than 10^{-5} of the suspension force in the axial direction - comparable to the end effects in the single wire case.

A related application is the proposed Equivalence Principle experiment. This is the intended application for these superconducting bearings; the experiment consists in comparing the motions of two test bodies falling around the earth (Fig. 18). The magnetic bearings constrain the masses to move along their common cylinder axis, and the satellite must be drag-free with respect to one of the masses to reduce perturbations from air drag and solar pressure. The mass positions are monitored by SQUID position detectors and they are shielded from electromagnetic disturbances by superconducting shields. A ground-based working model of the experiment is presently being funded by NSF,[9] and we have recently begun a study for NASA[10] to determine if the experiment can be done at reduced sensitivity on shuttle. Keeping in mind the considerations in section III.i. above, and a variety of other disturbances (ref. 2),

[8] F. F. Mobley, G. H. Fountain, A. C. Sadelik, P. W. Worden, R. A. Van Patten "Electromagnetic Suspension for the TIP-II Satellite", IEEE transactions on Magnetics, Vol. Mag-11, # 6, Nov., 1975.

[9] NSF Grant # PHY 78-23006: "A Cryogenic Equivalence Principle Experiment"

[10] NASA Contract # NAS8-33796: "A Preliminary Study of a Cryogenic Equivalence principle Experiment on Shuttle"

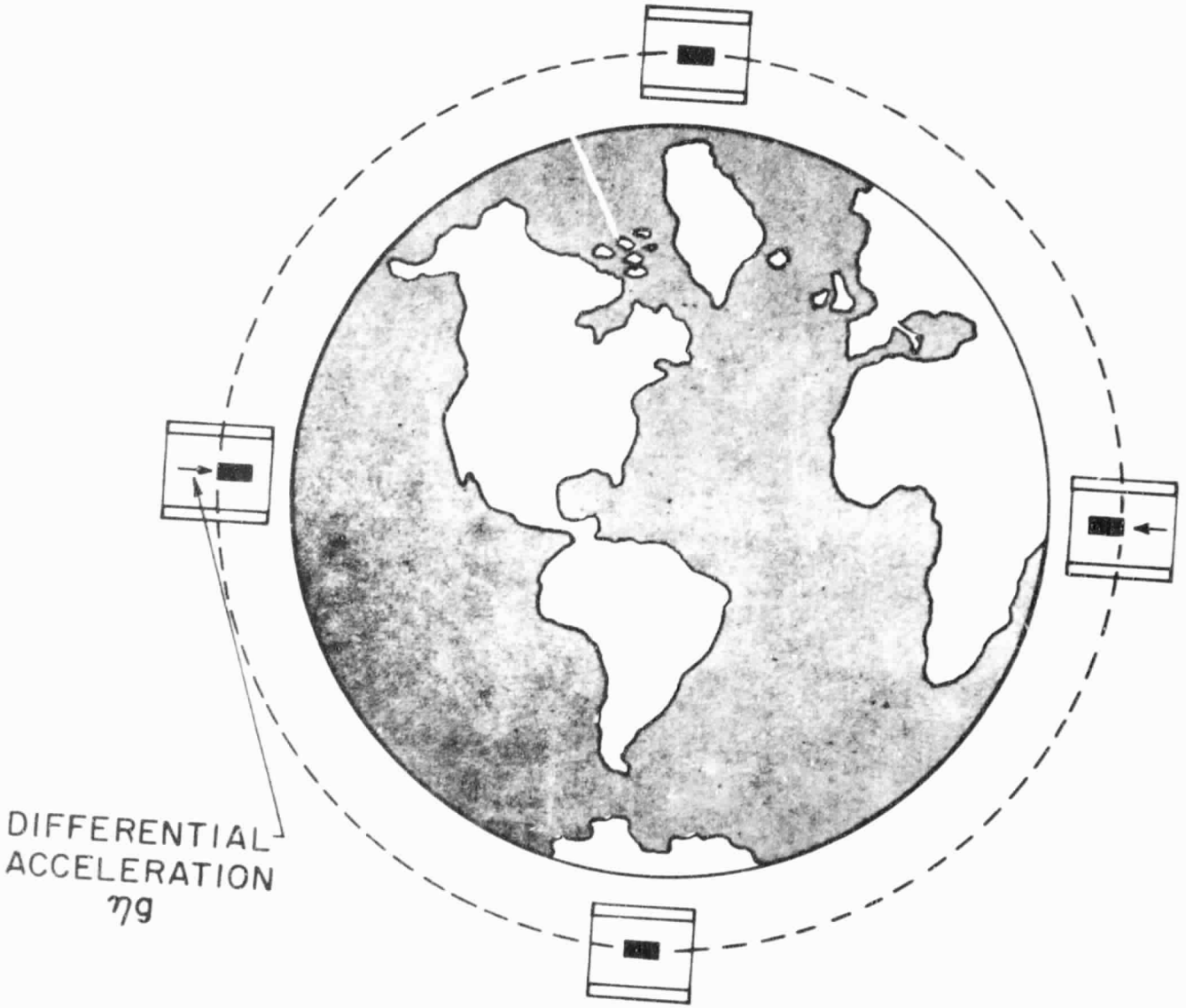

Figure 18

we believe that an orbital equivalence principle experiment, using bearings of about the same quality as we have demonstrated, can measure a difference in acceleration of two test bodies of one part in 10^{17}.

2) Accelerometers. We distinguish an accelerometer from a drag-free system by the forces which keep the test body in place relative to the spacecraft rather than the other way around. Spacecraft use accelerometers for several purposes: to supplement tracking data, monitor thrustor firings, gas drag and external disturbances. Practical accelerometers are single axis (Bell-Mesa) and three-axis types (CACTUS accelerometer)[11] and have electrical suspensions. The performance of these instruments is limited by electrical charging effects from cosmic rays, thermal gas pressure effects, surface effects and electronic noise. A superconducting bearing has the possibility of reducing the last three: the low temperature freezes out all but the lightest gases, surface potentials may be enormously reduced,[12] and advanced techniques applied to the position measurement.

A specific application for accelerometers made with superconducting bearings is in terrestrial and extraterrestrial gravity gradient mapping. Room temperature instruments for this purpose have been described.[13] A gravity gradiometer in a spacecraft consists of at least one accelerometer located at some distance from the center of mass of the spacecraft. In a nonuniform gravitational field the accelerometer tends to fall at a slightly different rate than the center of mass, but being restrained it registers an acceleration.

[11] J. Beaussier, A. M. Mainguy, A. Olivero, R. Rolland, "In Orbit performance of the CACTUS Accelerometer"

[12] J. M. Lockhart, F. C. Witteborn, W. M. Fairbank, "Evidence for a Temperature-Dependent Surface Shielding Effect in Cu", Phys. Rev. Letters 38, 21 (23 May, 1977).

[13] R. L. Forward, L. R. Miller, "Generation and detection of dynamic Gravitational-Gradient Fields", Journal of Applied Physics, Vol. 38 # 2, p. 512, Feb., 1967.

The spacecraft is spun to provide a periodic signal.

Superconducting accelerometers for study of gravity gradients are under development.[14] At present these use niobium masses suspended from diaphragms as test bodies and make up for the extra spring constant by very sensitive position detectors. A different optimization would lead to the opposite case, a mass freely suspended in a superconducting bearing with somewhat less sensitive position detectors. Bifilar bearings would be very good for this; alternatively a case could be made for a single wire suspension modelled after that of the TIP-III satellite. Several levitated-mass accelerometers have been developed or described in the literature.[15,16]

An accelerometer on the surface of a planet is a gravimeter or seismometer. Earth-based superconducting gravimeters of great sensitivity and stability are used to measure earth tides and motions.[17] Emplacement of a superconducting gravimeter on the moon could lead to important new information on the tidal interaction of the earth and moon, and tectonic information on other planets could likewise be collected.

3) mechanical systems. Obviously any moving part in a spacecraft is a candidate for a superconducting bearing. For most of these superconducting bearings are inappropriate for one or more of the reasons given above. We have found three applications in this area which are possibly practical provided the cryogenic environment is available for other reasons.

[14] H. J. Paik, "Superconducting tensor gravity gradiometer with SQUID Readout" Proc. conference on SQUID applications to Geophysics, Los Alamos, N.M., June 2-4, 1980. (In Press).

[15] P. K. Chapman, S. Ezekiel, Rev. Sci. Inst. 36, #1, p. 96 (1965).

[16] W. C. Oelfke, W. O. Hamilton, Acta Astronautica, Vol. 5, #1-2, p. 87-96, Jan. - Feb. 1978.

[17] Goodkind, J. M., "Continuous measurements with the superconducting gravimeter", Tectonophysics, Vol. 52 #1-4, pp. 99-105 (1979).

Despun or spinning sections of the spacecraft may be the most appropriate of these. Examples might be antennas or telescopes attached to a spin stabilized satellite. These would probably be bearings of type 4 in the appendix for two reasons: the greater load-bearing capacity and the possibility of using room temperature permanent magnets suspended near a superconductor. Thus the despun section is not necessarily cryogenic. The advantage of this sort of suspension would be essentially zero power consumption in maintaining the relative spin, and vibration isolation as well.

A related application might be to reaction wheels for controlling the attitude of a spacecraft. The principle advantages would be in low friction and small noise generation; some serious problems might be encountered in spinning up the wheels through the resonant frequency of the bearing.[18] Flywheels may also be used for energy storage, and it would be natural to reduce losses by making them superconducting.

A possible further application would be to attitude reference gyros, suspended so as to have minimum interaction with the spacecraft. The problem here is that perfectly good electrical suspensions exist, and any advantage would stem from a superconducting magnetic suspension being stable and requiring no external circuits.

We are aware of at least one case where a partially superconducting bearing would have been an appropriate suspension for a spinning mirror in a space experiment. This is in an experiment proposed by P. Boynton and others for spacelab II, to measure the anistropy of the cosmic background radiation using a bolometer, heat trap, and rotating mirror to scan a cone of sky. The preferred system for rotation required no mechanical contact. This could have been

[18] R. D. Bourke, "A Theoretical and Experimental Investigation of a Superconducting Magnetically-Supported Spinning Body", Stanford University Dept. of Aeronautics and Astronautics Report No. 189 (May 1964).

provided by an annular permanent magnet enclosed by a thin superconducting ring (type 4 suspension) and rotated by a rotating magnetic field.

4) General scientific applications. This group includes many experiments which are not yet at a stage where the precise application of superconducting bearings in a satellite might be stated, but in which their application is anticipated, and which might benefit from some aspect of a satellite environment such as weightlessness or low vibration environment. Examples include non-geodesic motion of spinning bodies (P. K. Chapman), measurements of the rate of change of the gravitational constant (R. Ritter), several "laboratory" tests of general relativity (V. B. Braginsky, K. Thorne, C. W. F. Everitt, C. Caves) and possibly gravitational wave experiments. These and others are discussed in [19] as well as a recent article[20].

In other examples the application is less directly related to the experiment itself but is possibly required for the supporting technology. An example might be studies of superfluid helium in a weightless environment. A study of superfluid He^3 would require a dilution refrigerator to reach a low enough temperature; the refrigerator in turn requires gravity to achieve a phase separation. Gravity could only be provided in an otherwise weightless environment by a centrifuge of some sort, and a low-vibration, low-heat generation superconducting bearing would be ideal for this.

[19] C. W. F. Everitt, "Feasibility analysis of Gravitational Experiments in Space", W. W. Hansen Laboratories of Physics, Stanford, CA (Sept. 1977).

[20] R. L. Peterson, "Space Applications of SUperconductivity: Instrumentation for gravitational and related studies", Cryogenics, Vol. 20 #6, p. 299-306 (June 1980).

VII. SUMMARY AND CONCLUSIONS

This report summarizes research conducted since mid-1977 on superconducting magnetic bearings for general application in space, with particular emphasis on a linear bearing of very high quality and low dissipation for a proposed equivalence principle experiment. The bearing is made with a bifilar winding consisting of a single wire doubled back on itself and wound as one wire; this provides the stiffest support possible with negligible fringing fields. We have constructed a version of the bearing which appears to be suitable for the equivalence principle experiment: its deviation from perfect straightness, measured by the second derivative of the height of the levitated mass, is less than our present sensitivity of roughly 1×10^{-4} cm^{-1} over the range of motion. This is a factor of 100 improvement over previous versions of the bearing.

We have also reviewed selected potential applications of the bearings in space. From the available literature we believe the most important general categories of use will be in gravitational experiments (which often must use superconducting technology anyway) and in gravimetry (which can benefit greatly from the stability and sensitivity of superconducting accelerometers).

APPENDIX I

I. Magnetic bearing types

For completeness we will summarize here the different magnetic bearing types and properties. We have identified four main categories which we have further subdivided into superconducting and non-superconducting types.

1) Diamagnetic bearings. These are the simplest type as regards construction and operation, consisting only of a piece of intrinsically diamagnetic material and some sort of magnet configured to produce a local minimum in the field intensity. The diamagnet develops an induced moment such that it is attracted to the minimum. The forces that can be produced are small even for strongly diamagnetic materials such as graphite.

2) Induced current bearings. A magnet near a superconductor induces image currents in it which prevent the field entering the superconductor. The superconductor therefore behaves as if it were perfectly diamagnetic, and experiences a force in the direction of the field gradient, exactly as in case a). The force in this case may be large enough to lift massive bodies. The room temperature equivalent uses an alternating magnetic field which is excluded from an ordinary conductor to the extent that the skin depth is small. The RMS force is at most half of the DC case, however, and because the induced currents die out rapidly in resistive materials, high frequencies and large powers are required. Only limited room temperature applications have been found. Types a) and b) are intrinsically stable, that is, the levitated mass tends to oscillate about an equilibrium position.

3) ferromagnetic bearings. In these a piece of magnetic material is attracted to an electromagnet. As the magnetic material approaches, the current to the electromagnet is cut off with appropriate phase shifts to provide stability. In the absence of external forces two or more electro-

magnets may be required unless the material is permanently magnetized. Many variations exist and large forces are possible. These bearings are stable only because of the controller for the electromagnet.

4) mixed ferromagnetic and induced current. The best examples work with superconductors. Suppose a superconducting sheet is cooled through its transition temperature with a piece of magnetized material nearby. The magnetic field becomes trapped in the superconductor below the transition, and if the magnet is moved in any direction from its original position, currents are induced in the superconductor which oppose the motion. The same can be done entirely with superconductors, but the ferromagnetic material can substantially increase the forces. This is an intrinsically stable situation. A room temperature example is an AC electromagnet whose impedance is changed by the presence of a magnetic slug. In a resonant circuit the current may be arranged to change in such a way that the slug has a stable position (at least when acted on by an external force).

II. Previous Research on Magnetic Bearings and on Rotating Superconducting Machinery

The principle of magnetic levitation of superconductors has been known for a long time and made the subject of laboratory demonstrations since the early 1950's. The frontispiece of D. Shoenberg's Superconductivity (Cambridge, 1957), for example, illustrates a permanent magnet floating above a superconducting dish. Despite this early work surprisingly little research has been done on superconducting bearings for technological application.

The early 1960's saw two programs to develop magnetically supported superconducting gyroscopes at the General Electric Company (Principal Investigator: T. A. Buchold) and at the Jet Propulsion Laboratory (Principal Investigator: J. Harding). Neither had much success. The Stanford Gyro Relativity Experi-

ment (Principal Investigators: W. M. Fairbank, C. W. F. Everitt, D. B. DeBra) was originally conceived as a magnetically levitated gyroscope with Mossbauer readout but with the conception of the London moment readout, magnetic suspension of the gyroscope was abandoned in favor of electrical suspension using a principle that had been invented by the late Arnold Nordsieck of the University of Illinois and engineered by Honeywell Incorporated.

An excellent theoretical paper: "The Magnetic Forces on Superconductors and Their Applications for Magnetic Bearings"[21] was written by T. A. Buchold in 1960 but the designs described there seem never to have been reduced to practice and the work was dropped when the General Electric superconducting gyroscope program was cancelled.

Recent years have seen new interest in large scale superconducting machinery applied to superconducting generators and the superconducting train. The superconducting train employs a magnetic levitation system of type II based on a different principle. The train carries a series of high field superconducting magnets and runs over a flat aluminum track. At low speeds it is supported on wheels but as the train accelerates it reaches a speed where the repulsive force between the moving magnet and the eddy currents in the track causes levitation.[22,23] Thus the bearing is inherently dissipative; the function of the superconducting magnet is simply to provide a high enough magnetic field for levitation to take place at a reasonable speed. References 22 and 23 are two representative papers in this field.

[21] Cryogenics 2, 203 (1961)

[22] Homer, G. J., Randle, T. C., Walters, C. R., Wilson, M. S. and Bevir, M. K. "A New Method for Stable Levitation of an Iron Body Using Superconductors" (Rutherford Laboratory paper, CR7676).

[23] Wipf, S. L., Cryogenics 16, 281-288 (1976).

Superconducting generators are being developed at M.I.T. and in several industrial companies.[24] They substitute a rotating superconducting magnet for the armature winding of the conventional generator to take advantage of the high field densities available with superconducting magnets. The result is a unit 60% the size of a conventional generator of the same output, with the ultimate possibility of increasing the size limit on commercial generators by a factor of two without facing the horrible difficulties of assembly at the site. In principle a superconducting generator could use superconducting bearings of the kind described here, but so far there has been little pressure to do so because a transition to room temperature has to be made anyway at some point to couple the generator to the power source. The approaches therefore have been to use room temperature bearings with either the entire dewar rotating or with vacuum rotary seals between the shaft and a chamber containing the superconducting magnet.

Magnetic levitation of a rotating superconductor has been applied in a few specialized physics experiments, for example, the research done by K. Pickar at the University of Pennsylvania in 1962 and 1963 on the helium flux thickness on a horizontal rotating disk [25], and the experiments on helium films done by Wang and Petrack at JPL using the rotor of Harding's cryogenic gyroscope.[26] Other applications include the work of Goodkind and his associates and of

[24] References to the enormous literature are available from the Electric Power Research Institute and NBS Surveys of Superconductors and Superconducting Devices.

[25] K. Pickar, University of Pennsylvania Ph.D. thesis, 1964. This research was a development of the work of Pickar and Everitt on third sound in moving helium films.

[26] T. Wang and B. Petrack

Tuman[27] on superconducting accelerometers.

The most interesting dynamical study of superconducting bearings was the research undertaken by R. D. Bourke in the Stanford Department of Aeronautics and Astronautics during the early stages of the Gyro Relativity program.[28] Bourke investigated stability criteria for a mushroom-shaped rotating superconductor supported magnetically and spinning at speeds up to 40 Hz and developed a technique for accelerating it through a region of instability by switching the magnetic field levels.

Another important application of magnetic levitation is to the Stanford/Louisiana State University/University of Rome gravitational wave antenna. In these devices a massive aluminum bar weighing ten tons is coated with superconductor and levitated over superconducting magnets.[29] The goal is to supply a levitation system of low spring constant for vibration isolation. Magnetic bearings provide an ideal 2-pole filter in contrast to mechanical systems which always have transmission at several frequencies.

The bearings described in this report differ markedly from any described above, except those studied theoretically by Buchold. They are specifically designed to provide extremely stiff lateral support for shafts or cylindrical test bodies. They have small clearances to maintain accurate centering; they utilize persistent current magnets for support; they have extremely low dissipation.

[27] V. S. Tuman, Nature 229, 618 (1971).

[28] Bourke, R. D., A Theoretical and Experimental Study of a Magnetically-Supported Spinning Body (Stanford University Ph.D. Thesis, 1964) SUDAAR #189.

[29] Boughn, S. P., The Design and Construction of a Cryogenic Gravitational Wave Detector (Stanford University Ph.D. Thesis, 1975) (HEPL Report # 764), Chapter 6.